

# **A Review of Two-Dimensional Liquid Chromatography Approaches Using Parallel Column Arrays in the Second Dimension**

Samuel W. Foster<sup>1</sup>, Deklin Parker<sup>1</sup>, Sangeeta Kurre<sup>1</sup>, John Boughton<sup>1</sup>, Dwight R. Stoll<sup>2</sup>,  
James P. Grinias<sup>1,\*</sup>

<sup>1</sup> Department of Chemistry & Biochemistry, Rowan University, 201 Mullica Hill Rd., Glassboro, NJ 08028 USA

<sup>2</sup> Department of Chemistry, Gustavus Adolphus College, 800 West College Avenue, Saint Peter, MN 56082 USA

\*Corresponding Author: James P. Grinias, [grinias@rowan.edu](mailto:grinias@rowan.edu)

## Abstract

Multi-dimensional liquid chromatography techniques play an important role in the analysis of complex mixtures. The keys to maximizing peak capacity in these methods are fast sampling rates and sufficient complementarity between the first- ( $^1\text{D}$ ) and second- ( $^2\text{D}$ ) dimension separations. One way that these criteria have been met is by using  $^2\text{D}$  parallel column arrays. This review covers demonstrations of this approach in the literature that have been published over the past three decades. Two or more identical  $^2\text{D}$  columns can be operated in a sequential order to permit increased separation times and higher peak capacities in the second dimension without the concomitant decrease in sampling rate. The parallel column arrays can also be operated simultaneously to reduce total analysis time. Columns with different stationary phase chemistries can be used in the  $^2\text{D}$  column array to increase complementarity by utilizing specific stationary phases for various first dimension fractions. More recently, this type of platform has been used to automate the development of two-dimensional (2D) achiral-chiral LC methods. These strategies, as well as recent efforts towards the development of integrated, spatial multi-dimensional LC devices that include parallel column arrays, are discussed here.

**Keywords:** two-dimensional liquid chromatography, 2D-LC, multi-dimensional liquid chromatography, parallel column arrays, method development

32 **1. Introduction**

33 Maximizing separation peak capacity is a critical aspect of the analysis of complex mixtures by  
34 liquid chromatography (LC). However, there are practical limits to the peak capacity that can be obtained  
35 in one-dimensional separations given constraints based on the maximum achievable pressure (based on  
36 both system and column) and the time needed to perform the separation [1]. Because of these limits, multi-  
37 dimensional separation techniques have become an increasingly popular approach to the separation and  
38 analysis of complex mixtures.

39 Multi-dimensional liquid chromatography relies upon the use of two or more complementary  
40 separations (*i.e.* the separation mechanisms are completely independent from each other, also referred to  
41 as “orthogonal”) to enhance the resolution of analytes that cannot be isolated using a single separation  
42 mode. It is a powerful tool because the total peak capacity of the comprehensive multi-dimensional method  
43 is the product of the peak capacity of each individual separation. However, this relationship only holds  
44 true if (1) the dimensions are completely complementary (complete usage of the two-dimensional  
45 separation space), and (2) there is sufficient sampling of the preceding dimension’s separation into the  
46 subsequent dimensions (*i.e.* at least four samples across a peak bandwidth of eight standard deviations  
47 [2]). The first condition can be somewhat difficult to achieve because separation modes that are compatible  
48 for coupling often have some overlap between retention/elution behavior based on molecular size,  
49 polarity, and/or charge. The second requires very fast separations in the latter dimensions so that resolution  
50 obtained in a given separation is not lost in the transfer of fractions to the subsequent dimension. A number  
51 of review articles have focused on various aspects of column selection, method development, and  
52 hardware design in multi-dimensional LC approaches designed to achieve higher peak capacity [3–10].

53 The central theme of this review article is the use of multiple second-dimension ( $^2\text{D}$ ) columns to  
54 increase complementarity and/or sampling rate compared to the use of a single  $^2\text{D}$  column. These columns  
55 are typically arranged in parallel arrays, and such arrays previously been used in one-dimensional LC  
56 separations to either improve analytical throughput [11–20][21–23], increase method selectivity by using  
57 multiple stationary phases [24–33][34], or increase sample loadability by splitting the injected volume  
58 onto multiple columns [35]. Although the term “parallel” has been used to describe both instrument  
59 features and gradient method design in the multi-dimensional LC literature to date, the term is specifically  
60 used in this article to designate system designs in which more than one column is connected to the same  
61 incoming sample/eluent stream. In these arrays, the columns are operated in either an (1) alternating, (2)  
62 sequential, or (3) simultaneous way. To improve sampling rates while also potentially increasing the  $^2\text{D}$

63 peak capacity ( $n_c$ ), multiple columns with the same stationary phase can be operated in a  $^2$ D column array.  
64 To increase complementarity, multiple columns with different stationary phases can be employed to utilize  
65 more of the two-dimensional (2D) separation space and achieve higher peak capacities. In this review  
66 article, we will discuss recent demonstrations of both strategies, as well as describe how they have been  
67 applied to improve the capabilities of 2D-LC separations.

68

## 69 **2. Second-Dimension Column Arrays Using Identical Stationary Phases**

70 *2.1 Parallel Column Arrays Operated in an Alternating or Sequential Order*

71 Early experimental demonstrations of  $^2$ D dual-column arrays that were operated alternately to  
72 separate each eluted first-dimension ( $^1$ D) fraction focused on the analysis of chiral compounds. Originally,  
73 a serial arrangement of achiral and chiral columns was applied for the analysis of the cancer drug  
74 leucovorin (administered as a diastereomeric mixture) and its metabolite, 5-methyltetrahydrofolate [36].  
75 However, poor chromatographic efficiency on the chiral column led to broad peaks, which prevented  
76 extending the validated quantitation range of the drug in plasma below 1  $\mu$ g/mL. To improve the  
77 technique, they switched the order of the columns, and sent two heart-cut fractions from a  $^1$ D chiral  
78 separation to two independent  $^2$ D achiral C18 columns (**Figure 1**) [37]. Peaks were refocused at the head  
79 of the  $^2$ D columns and further separated from co-eluting compounds (full method described in **Figure 1**  
80 caption), building upon a similar approach that used two C18 trapping columns for modulation between  
81 the chiral and achiral separations [38]. The peak refocusing on the  $^2$ D columns extended the lower end of  
82 the validated range to 25 ng/mL, permitting extended pharmacokinetic studies to measure drug clearance  
83 over longer time periods [37]. This foundational work demonstrated how this type of  $^2$ D column  
84 arrangement could be used to facilitate improved 2D-LC separations by analyzing each heart-cut fraction  
85 on a separate column.

86 The next significant advances in this dual column approach came several years later, focusing on  
87 the development of comprehensive techniques for biomolecular analysis. For size-exclusion  
88 chromatography (SEC)  $\times$  reversed phase (RP) LC analysis of peptides from trypsin-digested proteins,  
89 several SEC columns were connected in series, with the outlet of the final column connected to a  $^2$ D dual-  
90 column array controlled by two four-port valves (**Figure 2**) [39]. A higher flow rate of 1 mL/min was  
91 used for the first 40 min of the separation to enable compounds to elute through the large volume SEC  
92 columns, followed by a drop to 0.1 mL/min for 140 min to perform comprehensive analysis on 35 fractions  
93 (cycle time on the  $^2$ D columns was 4 min, including a 3 min gradient and 1 min equilibration). This

94 approach achieved  $n_c$  of 495, which was a more than ten-fold improvement from approximate one-  
95 dimensional  $n_c$  values of 45 that were common at the time. To further improve the sensitivity of the  
96 technique, the internal diameter of the  $^2$ D RP columns was reduced from 4.6 mm to 1.0 mm [40]. Finally,  
97 to extend the system to the analysis of whole proteins from a cell lysate, the  $^2$ D columns were replaced  
98 with polymeric perfusion-style particles and directed to a UV absorbance detector followed by a fraction  
99 collector [41]. Fractions of interest were further characterized with off-line MS analysis performed  
100 through both ESI and MALDI ionization modes.

101 In the early 2000s, a series of reports were published focusing on the combination of  $^1$ D ion-  
102 exchange (IEX) separations with  $^2$ D RP column arrays for protein analysis. With a 10-port single valve  
103 modulator, both weak-anion exchange (WAX) [42] and strong-cation exchange (SCX) [43]  $^1$ D separations  
104 were coupled to a dual-column array of short 4.6 mm x 14 mm columns packed with 1.5  $\mu$ m non-porous  
105 silica particles bonded with C18 for rapid  $^2$ D RP separations. Twenty fractions (60 s each) were collected  
106 during a 20 min separation of a mixture of 11 intact proteins, with an estimated maximum  $n_c$  of 600.  
107 System capabilities were later increased through the addition of an in-line, size-based sample preparation  
108 step using a restricted access material (RAM) column prior to the first dimension IEX column, and an  
109 increase in the number of RP columns in the  $^2$ D array from two to four (**Figure 3**) [44]. Here, a 96 min  $^1$ D  
110 separation was fractionated into twenty-four 4 min fractions. Each  $^2$ D RP column went through a 16 min  
111 cycle of sample loading (4 min), elution (8 min), and column regeneration (4 min), with the entire process  
112 controlled using three 10-port valves. This approach was an early demonstration increasing the  $^2$ D  $n_c$ , and  
113 thus the overall  $n_c$ , while still maintaining sufficient fractionation sampling rates by utilizing a multiple  
114  $^2$ D column array. For the analysis of a human hemofiltrate sample primarily consisting of peptides and  
115 small proteins, the increased  $^2$ D  $n_c$  value of 130 provided a total calculated  $n_c$  of 3000 (based on 24  
116 fractions) for the 2D method. This platform was later applied for the identification of peptides in a similar  
117 sample matrix obtained from patients with chronic renal failure [45].

118 Various other reports using two or more identical  $^2$ D columns have also focused on protein and/or  
119 peptide separations. Using capillary-scale monolithic columns, IEX was coupled to a  $^2$ D array of three RP  
120 columns for the separation of intact proteins [46]. In this array, one column was being loaded with effluent  
121 from the  $^1$ D IEX column, another was being equilibrated with a starting condition solution (or washed to  
122 remove salts if sample was already loaded), and the third had the RP gradient method running for  
123 separation and elution of proteins. The full cycle time for a single  $^2$ D column to go through these sequential  
124 steps was 45 min. Fractions eluted from the  $^2$ D column were collected following the separation of an *E.*

125 *coli* lysate, and although most still contained multiple proteins, each fraction was found to contain 10 or  
126 fewer proteins (as shown by SDS-PAGE), thus greatly reducing the complexity of the original sample. To  
127 increase the frequency at which fractions could be collected while not reducing the <sup>2</sup>D analysis time to  
128 avoid loss of  $n_c$ , an additional switching valve was added and the number of <sup>2</sup>D columns was increased to  
129 twelve (**Figure 4**) [47]. Over 500 differentiated peaks were identified using the system with three <sup>2</sup>D  
130 columns and the number exceeded 900 when twelve <sup>2</sup>D columns were used. Absorbance detection was  
131 employed in both studies, with three individual detectors used with the smaller column array and a novel  
132 capillary-scale detector array [48] implemented for the twelve column set. In another approach, a <sup>1</sup>D WAX  
133 column was connected to two 4.6 mm x 50 mm C18 RP columns for alternate modulation of <sup>1</sup>D fractions  
134 [49]. To increase the overall  $n_c$ , the <sup>2</sup>D column connected to the <sup>2</sup>D pump for elution was also connected  
135 to a second, identical column in series for a combined <sup>2</sup>D column length of 100 mm. For the analysis of a  
136 tryptic digest of a four protein mixture,  $n_c$  of 650 was obtained. When the second 50 mm column in the  
137 <sup>2</sup>D serial arrangement was heated to 80°C to decrease the <sup>2</sup>D separation time, the number of analyzed  
138 fractions increased from 25 to 37, reducing undersampling and increasing  $n_c$  to 890.

139 To expand the technique to the use of normal phase (NP) LC  $\times$  RPLC with a <sup>2</sup>D dual column array,  
140 a modulation approaching using two 10-port valves was developed [50]. The first valve operated similarly  
141 to a typical 2D-LC modulation valve with two sample loops between dimensions, while the second valve  
142 enabled selection between the two <sup>2</sup>D columns (each connected to their own independent pumping system)  
143 for alternating operation. When coupling a 1.0 mm x 250 mm NP diol column to two parallel 4.6 mm x  
144 50 mm RP columns, a 1 min sampling time was achieved with the two <sup>2</sup>D columns each having a 2 min  
145 full cycle time. For the total 25 min analysis time of a small molecule test mixture,  $n_c$  of 487 was obtained  
146 (**Figure 5**), which was close to the theoretical maximum product value of each dimension based on the  
147 high complementarity between dimensions. When the <sup>1</sup>D separation time was extended to 90 min for the  
148 analysis of a lemon oil sample, the observed  $n_c$  was 1,095, which was more than double the value achieved  
149 with a traditional modulation approach using a single <sup>2</sup>D column. Lower effective  $n_c$  of 82 was observed  
150 for the analysis of a steroid sample using RPLC (cyanopropyl)  $\times$  RPLC (C18) with the same system  
151 because of the lower complementarity compared to NPLC  $\times$  RPLC. A follow-up study for the analysis of  
152 fish oil samples using the same columns showed similar losses due to poorer complementarity, with a  
153 theoretical  $n_c$  of 290 dropping to a calculated value of 159 when accounting for use of the 2D separation  
154 space [51]. For the analysis of tryptic peptide mixtures with a similar instrument setup, RPLC (low pH)  $\times$   
155 RPLC (high pH) was employed to increase complementarity even though RP columns were used in both

156 dimensions [52]. To achieve higher  ${}^1\text{D}$   $n_c$ , four 2.1 mm x 150 mm columns packed with sub-3  $\mu\text{m}$   
157 superficially porous C18 particles were coupled in series, while the second dimension employed 4.6 mm  
158 x 50 mm columns packed with 3.5  $\mu\text{m}$  fully porous C18 particles as in the previous work. With a 6 hr  
159 analysis time for the  ${}^1\text{D}$  separation, an effective  $n_c$  of 4,677 was observed, with the theoretical maximum  
160  $n_c$  diminished due to some undersampling of the narrow  ${}^1\text{D}$  peaks.

161 Several other applications have been demonstrated using 2D-LC techniques with parallel  ${}^2\text{D}$   
162 column arrays. To separate phenolic antioxidants and flavonoids, a method using complementary PEG-  
163 silica and Zr-Carbon phases in each dimension was developed [53]. A 10-port valve was used to alternate  
164 between the two 2.1 mm x 50 mm Zr-Carbon  ${}^2\text{D}$  columns. No assessment of peak capacity was reported,  
165 although high retention time repeatability was shown for the method (%RSD < 5%). Later, the same  ${}^2\text{D}$   
166 Zr-Carbon column array was coupled to a  ${}^1\text{D}$  C18 column for the analysis of beer and wine samples [54].  
167 The capability to operate the zirconia-based phases at higher temperatures up to 120°C allowed for higher  
168 throughput in the  ${}^2\text{D}$  separation that could be used in increase the overall sampling rate of the technique.  
169 For the analysis of ribosomal proteins from a yeast sample, a  ${}^1\text{D}$  SCX was performed using a step salt  
170 gradient followed by 18 min gradient RP separations on two alternating  ${}^2\text{D}$  C4 columns [55]. Other efforts  
171 relied upon monolithic columns with reduced flow resistance to achieve higher throughput  ${}^2\text{D}$  separations.  
172 An IEX  $\times$  RPLC separation of human urine metabolites utilized two  ${}^2\text{D}$  C18 monolith columns [56].  
173 Monolith columns have also been used for RPLC  $\times$  RPLC separations, with a  ${}^1\text{D}$  4.6 mm x 150 mm  
174 column packed with fully porous pentabromobenzyl-phase particles connected to two  ${}^2\text{D}$  4.6 mm x 50  
175 mm C18 silica monoliths [57]. The  ${}^2\text{D}$  columns were operated at an exceptionally high 16 mL/min flow  
176 rate to achieve a 12 s  ${}^2\text{D}$  separation time, which was then applied to the analysis of polycyclic  
177 aromatic hydrocarbons in gasoline extract samples. Other aromatic and polycyclic mixtures were separated with  
178 a modified column arrangement of a 4.6 mm x 150 mm fluorinated-alkyl column coupled to 4.6 mm x 30 mm  
179 C18 silica monoliths [58]. Here, additional valves containing sample loops were added to the modulator  
180 platform, permitting 15 s fractionation and a 30 s overall  ${}^2\text{D}$  separation time, with an observed  $n_c$  of 1190  
181 for a 65 min analysis. A summary of all of the experimental demonstrations of sequential  ${}^2\text{D}$  column  
182 operation in 2D-LC is provided in **Table 1**.

183 The theoretical foundation of the ability for  ${}^2\text{D}$  multi-column arrays to enhance the overall  $n_c$   
184 through this type of sequential operation relative to the use of a single column has been previously detailed  
185 [59]. Based on a series of calculations and simulations primarily dependent on the  ${}^2\text{D}$  cycle time, it was  
186 shown that increasing the number of columns in a  ${}^2\text{D}$  parallel array does increase  $n_c$ , albeit not linearly.

187 Because the increase in performance levels off as the number of columns increases, a practical limit of  
188 five columns in a  $^2$ D array was proposed. The more important advantage provided by these arrays was a  
189 reduction in the need for separations that meet minimum sampling time rates, easing the need for  
190 incredibly fast  $^2$ D cycle times. This is somewhat akin to current commercial instrumentation containing  
191 multiple stored injection loops that can be injected sequentially onto a  $^2$ D column [60] or previously  
192 reported research-based set-ups using 18 solid-phase extraction (SPE) cartridges instead of loops [61,62].  
193 The theoretical study does bring up a number of experimental factors that must be considered when setting  
194 up a parallel column array for 2D-LC, specifically in terms of column, tubing, and pump reproducibility  
195 to ensure that the exact same separation is being performed in each  $^2$ D column. This can be especially  
196 difficult to achieve in terms of identical columns, as even the best column manufacturers have slight  
197 column-to-column repeatability differences when using traditional slurry packing techniques. In practice  
198 as a research tool, especially when combined with MS detection, slight differences in the separations may  
199 not be as critical as they would be in a QA/QC environment. For these more quantitative applications, the  
200 complexity of instrumentation (especially in terms of the additional valves and control schemes that were  
201 required for most of the methods described in this section) and issues with exactly matching the  $^2$ D  
202 separations may preclude wide adoption of the technique.

203

#### 204 *2.2 Parallel Column Arrays Operated Simultaneously*

205 To reduce total analysis time, individual columns in  $^2$ D column arrays can be operated at the same  
206 time rather than sequentially. One approach to coupling a  $^1$ D SCX separation to 18  $^2$ D RP capillary LC  
207 columns was achieved through the combination of dual selector valves for fractionation and a micro-flow  
208 splitter to achieve simultaneous elution in the  $^2$ D column array (**Figure 6**) [63]. Each step change in the  
209  $^1$ D SCX salt gradient was fractionated onto a different  $^2$ D column by varying the position of the selector  
210 valves. Once all the fractions were loaded, an in-house fabricated 18-channel flow splitter was then used  
211 to send the mobile phase flow from a single pump to all 18  $^2$ D RP columns for concurrent 90 min gradient  
212 separations (180 min total separation time). The effluents from the  $^2$ D columns were deposited onto  
213 MALDI plates at 15 s intervals, providing 360 spots per column and a total of 6,480 spots for MALDI-  
214 TOF-TOF-MS off-line detection, which added an additional day to the total analysis time. In this original  
215 study, the MALDI matrix was added to each individual spot following the parallel LC elution, while a  
216 similar follow-up study using a 10-capillary  $^2$ D array included online mixing of a 1:1 addition of matrix  
217 to each effluent channel [64]. A modified set-up with a  $^1$ D SAX separation followed by an array of eight

218  $^2$ D analytical-scale RP columns that eluted into 96-well plates was applied for the identification of proteins  
219 from human plasma samples [65]. Following fractionation into the well plates (1 min fractions per  
220 channel, 0.2 mL total volume based on 0.2 mL/min flow rate, 110 total  $^2$ D separation time), a bicinchoninic  
221 acid assay was performed to identify which fractions contained high abundance proteins. The high  
222 abundance proteins were then removed from these fractions with an immunoaffinity protein depletion kit  
223 to improve detection of low abundance proteins when fractions were subsequently analyzed by nano-LC-  
224 MS/MS. Over 1,300 unique proteins were identified, with concentrations ranging from 0.01 ng/mL up to  
225 41 g/L in plasma [65]. A similar instrumental design and workflow that included an automated fraction  
226 collector [66] was more recently used to identify 4,436 proteins from HeLa cell extracts [67]. A summary  
227 of these methods is provided in **Table 2**. A limitation to most of these approaches was detection  
228 throughput, especially since many involved the use of off-line detectors. Multiplexed detection, such as  
229 the UV absorbance array described in [48] could reduce the total analysis time of simultaneous column  
230 operation. The disadvantage of this approach is that different detectors operating simultaneously may have  
231 slightly different signal response and would need to be calibrated individually, making effective  
232 quantitation more difficult to achieve.

233 Looking toward the future, the need for increasingly higher  $n_c$  to effectively analyze complex  
234 mixtures suggests adoption of higher-order multi-dimensional separation techniques, including three-  
235 dimensional (3D)-LC [68,69]. In spatial 3D-LC approaches that utilize integrated microfluidic devices to  
236 perform the separation, a core design component is the use of column arrays in the second and third  
237 dimensions that are operated simultaneously [70]. A foundational demonstration of this approach was an  
238 integrated microfluidic device that connected a  $^1$ D separation channel to a perpendicular spatial array of  
239 21  $^2$ D columns (**Figure 7**) [71]. This was later expanded to a 3D device that contained 16  $^2$ D channels and  
240 256 third dimension ( $^3$ D) channels [72]. A key consideration in these devices is flow distribution to ensure  
241 that mobile phase is effectively delivered to all channels in the column arrays. To optimize this process,  
242 several computational and experimental studies have focused on flow distributor designs in spatial multi-  
243 dimensional chromatographic devices [73–77]. Active control of these flow distributors to improve  
244 performance can be achieved through rotational confinement devices that can be used to quickly shift flow  
245 into perpendicular directions to modulate between dimensions [78,79] or with freeze-thaw valve actuation  
246 [80]. Further details on the design of these devices and potential approaches to detection for spatial 3D-  
247 LC separations were recently described by the Eeltink group [70]; interested readers are referred to this  
248 publication for more information.

250 **3. Second-Dimension Column Arrays Using Different Stationary Phases**

251 The concept of using multiple columns in a 2D-LC separation to expand the complementarity of  
252 the technique dates back to some of the earliest published discussions of the technique [81]. One of the  
253 key impediments to fully utilizing the 2D separation space is lack of complementarity, as coupling very  
254 distinct separation mechanisms can often be difficult due to incompatible mobile phase conditions [8].  
255 With a parallel array of <sup>2</sup>D columns each containing different stationary phases, the potential for expanding  
256 the complementarity between the dimensions increases. Experimental demonstrations of such an approach  
257 are summarized in **Table 3**. In the early 2000s, this strategy was demonstrated experimentally through the  
258 coupling of a single <sup>1</sup>D RP ODS-AQ column to parallel <sup>2</sup>D amino- and cyano-phase columns [82].  
259 Modulation to two different columns was controlled through a 12-port valve, with a variety of flow  
260 splitters and unions used to enable system operation with a single pumping system and a single in-line  
261 detector combination (PDA and MS). For the analysis of a mixture of various aromatic compounds, the  
262 <sup>1</sup>D fractions that contained co-eluting analytes were both able to be separated on the <sup>2</sup>D columns. The  
263 elution order was different on each column due to differences in stationary phase interactions for amine-  
264 containing compounds (**Figure 8**). The  $n_c$  of this approach was calculated at 450 for a 30 min total analysis  
265 time. For the separation of a mixture of barbiturates and other drug compounds, this same platform was  
266 used with a <sup>1</sup>D C18 column and two identical <sup>2</sup>D phenyl columns, allowing for a RPLC  $\times$  RPLC separation  
267 with some complementarity based on  $\pi$ - $\pi$  interactions with the phenyl phase [83]. The system was  
268 modified to utilize a separate pump for each dimension and a separate detector for each of two parallel <sup>2</sup>D  
269 columns [84]. In this case, two 4.6 mm x 20 mm mixed mode RP columns were used in the <sup>2</sup>D array. By  
270 using two different pumps, mobile phase conditions were selected that promoted separations based on <sup>1</sup>D  
271 hydrophobic interactions and <sup>2</sup>D ionogenic interactions in the mixed mode columns, providing  
272 complementarity for non-neutral compounds in the mixture. A different group later adopted this same  
273 instrument arrangement with two individual <sup>2</sup>D detectors, but implemented two identical 3.0 mm x 50 mm  
274 columns packed with sub-3  $\mu$ m core-shell materials for the <sup>2</sup>D array in a RPLC (low pH)  $\times$  RPLC (high  
275 pH) method [85]. The full cycle time for the <sup>2</sup>D gradient separation was 30 s, allowing for a sampling time  
276 of 15 s through the use of two columns. The method was successfully applied for the analysis of co-eluting  
277 pharmaceutical degradants and other minor components in an active pharmaceutical ingredient sample.

278 Multiple reports have described the use of complementary <sup>2</sup>D column arrays to aid in the separation  
279 of charged species. For the analysis of surfactant mixtures, a <sup>1</sup>D NP separation using a 1.0 mm x 250 mm

280 diol column was coupled to a <sup>2</sup>D array that contained a 4.0 mm x 125 mm C4 column and a 4.0 mm x 250  
281 mm C2 column [86]. Four heart-cut fractions were collected, with valve timing selected to elute the first  
282 fraction containing cationic and amphoteric species and the third fraction containing anionic sulfate  
283 species onto the C4 column. The second fraction containing nonionic species and the fourth fraction  
284 anionic sulfonate species were sent to the C2 column. The total analysis time was 54 min and detection  
285 limits as low as 10 ng on-column were observed using evaporative light scattering detection (ELSD). A  
286 2D-ion chromatography (IC) method has also been reported in which two <sup>2</sup>D columns (cation- and anion-  
287 exchange, respectively) are used to separate both cations and anions following fractionation on a <sup>1</sup>D trap  
288 column [87]. The combined method was used to separate and detect seven inorganic anions and six  
289 inorganic cations in a single injection, with detection limits in the 1 – 300 ppb range achieved using  
290 conductivity detection.

291 Systems using different phases within the <sup>2</sup>D column array have been used for a number of other  
292 specific applications requiring 2D separations. An aforementioned dual C18 silica monolith column array  
293 was modified to increase dimensional complementarity by replacing one of the <sup>2</sup>D columns with a  
294 pentabromobenzyl silica monolith [58]. Because the <sup>2</sup>D columns were operated in an alternating fashion,  
295 two complete analyses were needed to obtain a separation on each <sup>2</sup>D column (e.g. odd <sup>1</sup>D fractions would  
296 elute onto the C18 monolith in run one and even <sup>1</sup>D fractions would elute onto the C18 monolith in run  
297 two), doubling the total analysis time. A hydrophilic interaction (HILIC)-RPLC method for the  
298 identification of 12 small molecules in tartary buckwheat samples used a <sup>1</sup>D mixed-mode HILIC column  
299 and two different <sup>2</sup>D RP columns (phenyl and polar embedded phases) [88]. Although not comprehensive,  
300 the high selectivity of the method did permit quantitation of the similar analytes of interest, which are  
301 difficult to separate with 1D or less complementary 2D separations. For combined metabolomic and  
302 lipidomic methods in a single analysis, a short <sup>2</sup>D trap column separated polar metabolites from more  
303 hydrophobic metabolites and lipids, with each fraction diverted to a different <sup>2</sup>D RP column for sequential  
304 analysis [89]. More than 3200 features were observed in the analysis of a pooled human plasma sample,  
305 which is nearly identical to the summed features of independent metabolomic and lipidomic analyses;  
306 98.8% of the features identified in the combined method were the same as the two individual runs. This  
307 methodology was later applied to the analysis of acyl-CoAs in mutated glioma cells [90] and serum  
308 samples from esophageal squamous cell carcinoma patients [91]. A multi-detector approach for the  
309 lipidomic analysis of triacylglycerols in adult/infant formula has also been reported, with non-aqueous RP  
310 methods being used in both dimensions (<sup>1</sup>D C18 column and two C30 columns with different lengths in

311 the  $^2\text{D}$  array) [92,93]. The eluent from the  $^1\text{D}$  column first passed through in-line UV absorbance and FLD  
312 detector flow cells, then to a flow splitter that separated flow five ways: to a CAD detector, APPI-MS,  
313 ESI-MS, and each of the  $^2\text{D}$  columns. The 50 mm length C30 column was connected to in-line UV and  
314 ESI-MS detectors, while the 100 mm length C30 column had a post-column split to ELSD and ESI-MS  
315 detectors. Sixteen analytes fell within the certified reference value ranges of a NIST standard for  
316 adult/infant formula out of nineteen targeted compounds, demonstrating a potential alternative to the  
317 standard GC-FID method. The need for multiple MS instruments in this platform may make it difficult  
318 for many to adopt based on cost and laboratory space requirements. Although different ionization sources  
319 were used for these studies, multi-emitter tip designs [94] or motorized stages [95] that can be used to  
320 connect different columns to the same MS inlet may be a feasible alternative.

321 The pharmaceutical industry has demonstrated the use of parallel  $^2\text{D}$  column arrays using column  
322 selection valves to empirically identify the most complementary column combinations as part of  
323 automated method development processes. To help improve the detection and identification of impurities  
324 and degradation products in pharmaceutical formulations, a  $^1\text{D}$  RP separation was coupled to a six-column  
325  $^2\text{D}$  array [96]. Some of the  $^2\text{D}$  columns were also RP but had slightly different selectivity, enabling the  
326 separation of a small impurity from the tail of the large active pharmaceutical ingredient peak observed in  
327 the first dimension. One of the columns in the  $^2\text{D}$  array was actually identical to the  $^1\text{D}$  column and was  
328 used for mobile phase additive exchange from phosphate buffer to formic acid to enhance MS detection.  
329 Finally, an inorganic salt impurity was separated and detected by using a  $^2\text{D}$  HILIC column coupled to a  
330 charged aerosol detector. A similar instrument setup was later utilized for 2D achiral-chiral separations  
331 with a chiral column array in the second dimension (**Figure 9**) [97]. For method screening, each relevant  
332  $^1\text{D}$  heart-cut peak could be held in a sample loop and then a small aliquot of each loop could be sent to six  
333 different  $^2\text{D}$  columns to identify which chiral phase provided the highest resolution. Once the best chiral  
334 column from the array was identified for each peak, single methods could then be designed that sent each  
335 compound to a different column to ensure chiral separation, a feat that is very difficult to achieve when  
336 only a single  $^2\text{D}$  chiral column is used in a 2D achiral-chiral method. This is especially valuable for  
337 compounds with multiple chiral centers. To further automate method development for achiral-chiral peak  
338 purity analysis, column selection valves have been used for both  $^1\text{D}$  RP and  $^2\text{D}$  chiral column arrays, along  
339 with a mobile phase selector to screen additives for the achiral separation [98]. For the analysis of complex  
340 biopharmaceutical mixtures, automated method screening using the dual array platform employed  $^1\text{D}$   
341 SEC, IEX, and RP columns and a variety of  $^2\text{D}$  RP columns was demonstrated on a standard protein

342 mixture [99]. More recently, <sup>2</sup>D column arrays have been used for the automated characterization of  
343 multiple monoclonal antibody structural attributes [100]. These platforms utilizing parallel column arrays  
344 in the second dimension, and sometimes the first dimension as well, provide an automated approach to  
345 method development that can simplify the integration of 2D-LC into pharmaceutical purity and  
346 biopharmaceutical characterization analyses. Many of the examples in the preceding paragraphs of Section  
347 3 focused on methods developed for single applications, which may have less broad applicability.  
348 Automated pharmaceutical method development provides a much more likely area in which <sup>2</sup>D column  
349 arrays using columns with different stationary phases will be adopted.

350

#### 351 **4. Conclusions**

352 The collection of articles reviewed here highlight the various ways in which parallel column arrays  
353 can enhance multi-dimensional LC methods. The <sup>2</sup>D separation time can be extended while minimizing  
354 the effects on sampling rate and total analysis time when multiple identical column arrays are used.  
355 Simultaneous operation of multiple <sup>2</sup>D columns, especially at the capillary-scale or in integrated  
356 microfluidic devices, can also be performed to maximize <sup>2</sup>D throughput. Detection can be challenging for  
357 these approaches, but MALDI-MS detection of spatial arrays of eluted fractions can be utilized. When  
358 different stationary phases are used in <sup>2</sup>D column arrays, complementarity can be increased to better utilize  
359 the 2D separation space. This strategy is also becoming increasingly important for automated method  
360 screening in industry, especially when developing 2D achiral-chiral methods for pharmaceutical  
361 compounds. More traditional comprehensive 2D-LC techniques have increased in popularity with the  
362 wider availability of commercial solutions, both in terms of hardware and software. Further research  
363 building upon the multi-column approaches to improve 2D-LC performance described here, especially  
364 through higher complementarity based on the use of multiple stationary phases, may eventually increase  
365 the ubiquity of these methods as well. However, the complexity of instrumentation remains a barrier to  
366 wider adoption of this technique, and commercially available solutions may increase usage as has been  
367 observed with more traditional 2D-LC techniques.

368

#### 369 **Acknowledgements**

370 This work was supported by the Chemical Measurement and Imaging Program in the National  
371 Science Foundation Division of Chemistry under Grants CHE-2045023 (to JPG) and CHE-2003734 (to  
372 DRS).

373 **References**

374 [1] G. Guiochon, The limits of the separation power of unidimensional column liquid  
375 chromatography, *J. Chromatogr. A.* 1126 (2006) 6–49.  
376 <https://doi.org/10.1016/j.chroma.2006.07.032>.

377 [2] R.E. Murphy, M.R. Schure, J.P. Foley, Effect of Sampling Rate on Resolution in Comprehensive  
378 Two-Dimensional Liquid Chromatography, *Anal. Chem.* 70 (1998) 1585–1594.  
379 <https://doi.org/10.1021/ac971184b>.

380 [3] D.R. Stoll, X. Li, X. Wang, P.W. Carr, S.E.G. Porter, S.C. Rutan, Fast, comprehensive two-  
381 dimensional liquid chromatography, *J. Chromatogr. A.* 1168 (2007) 3–43.  
382 <https://doi.org/10.1016/J.CHROMA.2007.08.054>.

383 [4] P. Dugo, F. Cacciola, T. Kumm, G. Dugo, L. Mondello, Comprehensive multidimensional liquid  
384 chromatography: Theory and applications, *J. Chromatogr. A.* 1184 (2008) 353–368.  
385 <https://doi.org/10.1016/j.chroma.2007.06.074>.

386 [5] I. François, K. Sandra, P. Sandra, Comprehensive liquid chromatography: Fundamental aspects  
387 and practical considerations-A review, *Anal. Chim. Acta.* 641 (2009) 14–31.  
388 <https://doi.org/10.1016/j.aca.2009.03.041>.

389 [6] M. Iguiniz, S. Heinisch, Two-dimensional liquid chromatography in pharmaceutical analysis.  
390 Instrumental aspects, trends and applications, *J. Pharm. Biomed. Anal.* 145 (2017) 482–503.  
391 <https://doi.org/10.1016/j.jpba.2017.07.009>.

392 [7] D.R. Stoll, P.W. Carr, Two-Dimensional Liquid Chromatography: A State of the Art Tutorial,  
393 *Anal. Chem.* 89 (2017) 519–531. <https://doi.org/10.1021/acs.analchem.6b03506>.

394 [8] B.W.J. Pirok, A.F.G. Gargano, P.J. Schoenmakers, Optimizing separations in online  
395 comprehensive two-dimensional liquid chromatography, *J. Sep. Sci.* 41 (2018) 68–98.  
396 <https://doi.org/10.1002/jssc.201700863>.

397 [9] B.W.J.J. Pirok, D.R. Stoll, P.J. Schoenmakers, Recent Developments in Two-Dimensional Liquid  
398 Chromatography: Fundamental Improvements for Practical Applications, *Anal. Chem.* 91 (2019)  
399 240–263. <https://doi.org/10.1021/acs.analchem.8b04841>.

400 [10] J. De Vos, J.P. Grinias, D. Stoll, S. Buckenmaier, S. Eeltink, Advances in ultra-high-pressure and  
401 multi-dimensional liquid chromatography instrumentation and workflows, *Anal. Sci. Adv.* 2  
402 (2021) 171–192. <https://doi.org/10.1002/ansa.202100007>.

403 [11] L. Zeng, D.B. Kassel, Developments of a Fully Automated Parallel HPLC/ Mass Spectrometry

404 System for the Analytical Characterization and Preparative Purification of Combinatorial  
405 Libraries, *Anal. Chem.* 70 (1998) 4380–4388. <https://doi.org/10.1021/ac9805448>.

406 [12] V. De Biasi, N. Haskins, A. Organ, R. Bateman, K. Giles, S. Jarvis, High throughput liquid  
407 chromatography/mass spectrometric analyses using a novel multiplexed electrospray interface,  
408 *Rapid Commun. Mass Spectrom.* 13 (1999) 1165–1168. [https://doi.org/10.1002/\(SICI\)1097-0231\(19990630\)13:12<1165::AID-RCM638>3.0.CO;2-4](https://doi.org/10.1002/(SICI)1097-0231(19990630)13:12<1165::AID-RCM638>3.0.CO;2-4).

409 [13] W.A. Korfsmacher, J. Veals, K. Dunn-Meynell, X. Zhang, G. Tucker, K.A. Cox, C. Lin,  
410 Demonstration of the capabilities of a parallel high performance liquid chromatography tandem  
411 mass spectrometry system for use in the analysis of drug discovery plasma samples, *Rapid*  
412 *Commun. Mass Spectrom.* 13 (1999) 1991–1998. [https://doi.org/10.1002/\(sici\)1097-0231\(19991030\)13:20<1991::aid-rcm743>3.3.co;2-u](https://doi.org/10.1002/(sici)1097-0231(19991030)13:20<1991::aid-rcm743>3.3.co;2-u).

413 [14] D.L. Hiller, A.H. Brockman, L. Goulet, S. Ahmed, R.O. Cole, T. Covey, Application of a non-  
414 indexed dual sprayer pneumatically assisted electrospray source to the high throughput  
415 quantitation of target compounds in biological fluids, *Rapid Commun. Mass Spectrom.* 14 (2000)  
416 2034–2038. [https://doi.org/10.1002/1097-0231\(20001115\)14:21<2034::AID-RCM124>3.0.CO;2-6](https://doi.org/10.1002/1097-0231(20001115)14:21<2034::AID-RCM124>3.0.CO;2-6).

417 [15] C.K. Van Pelt, T.N. Corso, G.A. Schultz, S. Lowes, J. Henion, A four-column parallel  
418 chromatography system for isocratic or gradient LC/MS analyses, *Anal. Chem.* 73 (2001) 582–  
419 588. <https://doi.org/10.1021/ac0006876>.

420 [16] Y. Shen, N. Tolić, R. Zhao, L. Paša-Tolić, L. Li, S.J. Berger, R. Harkewicz, G.A. Anderson, M.E.  
421 Belov, R.D. Smith, High-throughput proteomics using high-efficiency multiple-capillary liquid  
422 chromatography with on-line high-performance ESI FTICR mass spectrometry, *Anal. Chem.* 73  
423 (2001) 3011–3021. <https://doi.org/10.1021/ac001393n>.

424 [17] M. Jemal, M. Huang, Y. Mao, D. Whigan, M.L. Powell, Increased throughput in quantitative  
425 bioanalysis using parallel-column liquid chromatography with mass spectrometric detection,  
426 *Rapid Commun. Mass Spectrom.* 15 (2001) 994–999. <https://doi.org/10.1002/rcm.330>.

427 [18] R.C. King, C. Miller-Stein, D.J. Magiera, J. Brann, Description and validation of a staggered  
428 parallel high performance liquid chromatography system for good laboratory practice level  
429 quantitative analysis by liquid chromatography/tandem mass spectrometry, *Rapid Commun. Mass*  
430 *Spectrom.* 16 (2002) 43–52. <https://doi.org/10.1002/rcm.539>.

431 [19] H. Wang, S.M. Hanash, Increased throughput and reduced carryover of mass spectrometry-based

435 proteomics using a high-efficiency nonsplit nanoflow parallel dual-column capillary HPLC  
436 system, *J. Proteome Res.* 7 (2008) 2743–2755. <https://doi.org/10.1021/pr700876g>.

437 [20] P. Diederich, S.K. Hansen, S.A. Oelmeier, B. Stolzenberger, J. Hubbuch, A sub-two minutes  
438 method for monoclonal antibody-aggregate quantification using parallel interlaced size exclusion  
439 high performance liquid chromatography, *J. Chromatogr. A.* 1218 (2011) 9010–9018.  
440 <https://doi.org/10.1016/j.chroma.2011.09.086>.

441 [21] A. Nagy, A. Gaspar, Packed multi-channels for parallel chromatographic separations in  
442 microchips, *J. Chromatogr. A.* 1304 (2013) 251–256.  
443 <https://doi.org/10.1016/j.chroma.2013.06.065>.

444 [22] J. Huft, C.A. Haynes, C.L. Hansen, Fabrication of high-quality microfluidic solid-phase  
445 chromatography columns, *Anal. Chem.* 85 (2013) 1797–1802. <https://doi.org/10.1021/ac303153a>.

446 [23] J. Huft, C.A. Haynes, C.L. Hansen, Microfluidic integration of parallel solid-phase liquid  
447 chromatography, *Anal. Chem.* 85 (2013) 2999–3005. <https://doi.org/10.1021/ac400163u>.

448 [24] G.M. Gross, B.J. Prazen, R.E. Synovec, Parallel column liquid chromatography with a single  
449 multi-wavelength absorbance detector for enhanced selectivity using chemometric analysis, *Anal.*  
450 *Chim. Acta* 490 (2003) 197–210. [https://doi.org/10.1016/S0003-2670\(03\)00669-X](https://doi.org/10.1016/S0003-2670(03)00669-X).

451 [25] Y. Wang, R. Lehmann, X. Lu, X. Zhao, G. Xu, Novel, fully automatic hydrophilic  
452 interaction/reversed-phase column-switching high-performance liquid chromatographic system  
453 for the complementary analysis of polar and apolar compounds in complex samples, *J.*  
454 *Chromatogr. A.* 1204 (2008) 28–34. <https://doi.org/10.1016/j.chroma.2008.07.010>.

455 [26] K. Klavins, H. Drexler, S. Hann, G. Koellensperger, Quantitative metabolite profiling utilizing  
456 parallel column analysis for simultaneous reversed-phase and hydrophilic interaction liquid  
457 chromatography separations combined with tandem mass spectrometry, *Anal. Chem.* 86 (2014)  
458 4145–4150. <https://doi.org/10.1021/ac5003454>.

459 [27] K. Ortmayr, S. Hann, G. Koellensperger, Complementing reversed-phase selectivity with porous  
460 graphitized carbon to increase the metabolome coverage in an on-line two-dimensional LC-MS  
461 setup for metabolomics., *Analyst*. 140 (2015) 3465–3473. <https://doi.org/10.1039/c5an00206k>.

462 [28] J. Robles-Molina, B. Gilbert-López, J.F. García-Reyes, A. Molina-Díaz, Simultaneous liquid  
463 chromatography/mass spectrometry determination of both polar and “multiresidue” pesticides in  
464 food using parallel hydrophilic interaction/reversed-phase liquid chromatography and a hybrid  
465 sample preparation approach, *J. Chromatogr. A.* 1517 (2017) 108–116.

466 <https://doi.org/10.1016/j.chroma.2017.08.041>.

467 [29] E. Rampler, H. Schoeny, B.M. Mitic, Y. El Abiead, M. Schwaiger, G. Koellensperger,  
468 Simultaneous non-polar and polar lipid analysis by on-line combination of HILIC, RP and high  
469 resolution MS, *Analyst*. 143 (2018) 1250–1258. <https://doi.org/10.1039/c7an01984j>.

470 [30] M. Schwaiger, H. Schoeny, Y. El Abiead, G. Hermann, E. Rampler, G. Koellensperger, Merging  
471 metabolomics and lipidomics into one analytical run, *Analyst*. 144 (2019) 220–229.  
472 <https://doi.org/10.1039/c8an01219a>.

473 [31] M.A.I. Prodhan, B. Shi, M. Song, L. He, F. Yuan, X. Yin, P. Bohman, C.J. McClain, X. Zhang,  
474 Integrating comprehensive two-dimensional gas chromatography mass spectrometry and parallel  
475 two-dimensional liquid chromatography mass spectrometry for untargeted metabolomics,  
476 *Analyst*. 144 (2019) 4331–4341. <https://doi.org/10.1039/c9an00560a>.

477 [32] F. Yuan, S. Kim, X. Yin, X. Zhang, I. Kato, Integrating two-dimensional gas and liquid  
478 chromatography-mass spectrometry for untargeted colorectal cancer metabolomics: A proof-of-  
479 principle study, *Metabolites*. 10 (2020) 343. <https://doi.org/10.3390/metabo10090343>.

480 [33] F. Yuan, J. Harder, J. Ma, X. Yin, X. Zhang, M.M. Kosiewicz, Using Multiple Analytical  
481 Platforms to Investigate the Androgen Depletion Effects on Fecal Metabolites in a Mouse Model  
482 of Systemic Lupus Erythematosus, *J. Proteome Res.* 19 (2020) 667–676.  
483 <https://doi.org/10.1021/acs.jproteome.9b00558>.

484 [34] M. Komendová, S. Nawada, R. Metelka, P.J. Schoenmakers, J. Urban, Multichannel separation  
485 device with parallel electrochemical detection, *J. Chromatogr. A*. 1610 (2020) 460537.  
486 <https://doi.org/10.1016/j.chroma.2019.460537>.

487 [35] M.J. Gray, P.J. Slonecker, G. Dennis, R.A. Shalliker, A column capacity study of single, serial,  
488 and parallel linked rod monolithic high performance liquid chromatography columns, *J.*  
489 *Chromatogr. A*. 1096 (2005) 92–100. <https://doi.org/10.1016/j.chroma.2005.06.091>.

490 [36] I.W. Wainer, R.M. Stiffin, Direct resolution of the stereoisomers of leucovorin and 5-  
491 methyltetrahydrofolate using a bovine serum albumin high-performance liquid chromatographic  
492 chiral stationary phase coupled to an achiral phenyl column, *J. Chromatogr. B Biomed. Sci. Appl.*  
493 424 (1988) 158–162. [https://doi.org/10.1016/S0378-4347\(00\)81088-9](https://doi.org/10.1016/S0378-4347(00)81088-9).

494 [37] L. Silan, P. Jadaud, L.R. Whitfield, I.W. Wainer, Determination of low levels of the stereoisomers  
495 of leucovorin and 5-methyltetrahydrofolate in plasma using a coupled chiral-achiral high-  
496 performance liquid chromatographic system with post-chiral column peak compression, *J.*

497 Chromatogr. B Biomed. Sci. Appl. 532 (1990) 227–236. [https://doi.org/10.1016/S0378-4347\(00\)83774-3](https://doi.org/10.1016/S0378-4347(00)83774-3).

498

499 [38] A. Walhagen, L.-E. Edholm, Coupled-column chromatography on immobilized protein phases for 500 direct separation and determination of drug enantiomers in plasma, J. Chromatogr. A. 473 501 (1989) 371–379. [https://doi.org/10.1016/S0021-9673\(00\)91321-9](https://doi.org/10.1016/S0021-9673(00)91321-9).

502 [39] G.J. Opiteck, J.W. Jorgenson, R.J. Anderegg, Two-Dimensional SEC/RPLC Coupled to Mass 503 Spectrometry for the Analysis of Peptides, Anal. Chem. 69 (1997) 2283–2291. 504 <https://doi.org/10.1021/ac961156d>.

505 [40] G.J. Opiteck, J.W. Jorgenson, M.A. Moseley, R.J. Anderegg, Two-Dimensional Microcolumn 506 HPLC Coupled to a Single-Quadrupole Mass Spectrometer for the Elucidation of Sequence Tags 507 and Peptide Mapping, J. Microcolumn Sep. 10 (1998) 365–375. 508 [https://doi.org/10.1002/\(SICI\)1520-667X\(1998\)10:4<365::AID-MCS6>3.0.CO;2-E](https://doi.org/10.1002/(SICI)1520-667X(1998)10:4<365::AID-MCS6>3.0.CO;2-E).

509 [41] G.J. Opiteck, S.M. Ramirez, J.W. Jorgenson, M.A. Moseley, Comprehensive two-dimensional 510 high-performance liquid chromatography for the isolation of overexpressed proteins and 511 proteome mapping, Anal. Biochem. 258 (1998) 349–361. <https://doi.org/10.1006/abio.1998.2588>.

512 [42] K.K. Unger, K. Racaityte, K. Wagner, T. Miliotis, L.E. Edholm, R. Bischoff, G. Marko-Varga, Is 513 multidimensional High Performance Liquid Chromatography (HPLC) an alternative in protein 514 analysis to 2D gel electrophoresis?, HRC J. High Resolut. Chromatogr. 23 (2000) 259–265. 515 [https://doi.org/10.1002/\(SICI\)1521-4168\(20000301\)23:3<259::AID-JHRC259>3.0.CO;2-V](https://doi.org/10.1002/(SICI)1521-4168(20000301)23:3<259::AID-JHRC259>3.0.CO;2-V).

516 [43] K. Wagner, K. Racaityte, K.K. Unger, T. Miliotis, L.E. Edholm, R. Bischoff, G. Marko-Varga, 517 Protein mapping by two-dimensional high performance liquid chromatography, J. Chromatogr. A. 518 893 (2000) 293–305. [https://doi.org/10.1016/S0021-9673\(00\)00736-6](https://doi.org/10.1016/S0021-9673(00)00736-6).

519 [44] K. Wagner, T. Miliotis, G. Marko-Varga, R. Bischoff, K.K. Unger, An automated on-line 520 multidimensional HPLC system for protein and peptide mapping with integrated sample 521 preparation, Anal. Chem. 74 (2002) 809–820. <https://doi.org/10.1021/ac010627f>.

522 [45] E. Machtejevas, H. John, K. Wagner, L. Ständker, G. Marko-Varga, W.G. Forssmann, R. 523 Bischoff, K.K. Unger, Automated multi-dimensional liquid chromatography: Sample preparation 524 and identification of peptides from human blood filtrate, J. Chromatogr. B Anal. Technol. 525 Biomed. Life Sci. 803 (2004) 121–130. <https://doi.org/10.1016/j.jchromb.2003.07.015>.

526 [46] Z. Zhu, H. Chen, J. Ren, J.J. Lu, C. Gu, K.B. Lynch, S. Wu, Z. Wang, C. Cao, S. Liu, Two- 527 dimensional chromatographic analysis using three second-dimension columns for continuous

528 comprehensive analysis of intact proteins, *Talanta*. 179 (2018) 588–593.  
529 <https://doi.org/10.1016/j.talanta.2017.11.060>.

530 [47] J. Ren, M.A. Beckner, K.B. Lynch, H. Chen, Z. Zhu, Y. Yang, A. Chen, Z. Qiao, S. Liu, J.J. Lu,  
531 Two-dimensional liquid chromatography consisting of twelve second-dimension columns for  
532 comprehensive analysis of intact proteins, *Talanta*. 182 (2018) 225–229.  
533 <https://doi.org/10.1016/j.talanta.2018.01.072>.

534 [48] K.B. Lynch, Y. Yang, J. Ren, S. Liu, Multiple-channel ultra-violet absorbance detector for two-  
535 dimensional chromatographic separations, *Talanta*. 181 (2018) 416–421.  
536 <https://doi.org/10.1016/j.talanta.2018.01.045>.

537 [49] D. Li, L. Zhang, Z. Wang, A. Intisar, W. Zhang, Development of a parallel-tandem column  
538 interface in a two-dimensional liquid chromatography system, *Chromatographia*. 73 (2011) 871–  
539 877. <https://doi.org/10.1007/s10337-011-1974-x>.

540 [50] I. François, A. de Villiers, B. Tienpont, F. David, P. Sandra, Comprehensive two-dimensional  
541 liquid chromatography applying two parallel columns in the second dimension, *J. Chromatogr. A*.  
542 1178 (2008) 33–42. <https://doi.org/10.1016/j.chroma.2007.11.032>.

543 [51] I. François, P. Sandra, Comprehensive supercritical fluid chromatography × reversed phase liquid  
544 chromatography for the analysis of the fatty acids in fish oil, *J. Chromatogr. A*. 1216 (2009)  
545 4005–4012. <https://doi.org/10.1016/j.chroma.2009.02.078>.

546 [52] I. François, D. Cabooter, K. Sandra, F. Lynen, G. Desmet, P. Sandra, Tryptic digest analysis by  
547 comprehensive reversed phase x two reversed phase liquid chromatography (RP-LC x RP-LC) at  
548 different pH's, *J. Sep. Sci.* 32 (2009) 1137–1144. <https://doi.org/10.1002/jssc.200800578>.

549 [53] F. Cacciola, P. Jandera, E. Blahová, L. Mondello, Development of different comprehensive two  
550 dimensional systems for the separation of phenolic antioxidants, *J. Sep. Sci.* 29 (2006) 2500–  
551 2513. <https://doi.org/10.1002/jssc.200600213>.

552 [54] F. Cacciola, P. Jandera, L. Mondello, Temperature effects on separation on zirconia columns:  
553 Applications to one- and two-dimensional LC separations of phenolic antioxidants, *J. Sep. Sci.* 30  
554 (2007) 462–474. <https://doi.org/10.1002/jssc.200600387>.

555 [55] H. Liu, S.J. Berger, A.B. Chakraborty, R.S. Plumb, S.A. Cohen, Multidimensional  
556 chromatography coupled to electrospray ionization time-of-flight mass spectrometry as an  
557 alternative to two-dimensional gels for the identification and analysis of complex mixtures of  
558 intact proteins, *J. Chromatogr. B Anal. Technol. Biomed. Life Sci.* 782 (2002) 267–289.

559 [https://doi.org/10.1016/S1570-0232\(02\)00554-8](https://doi.org/10.1016/S1570-0232(02)00554-8).

560 [56] S.P. Dixon, I.D. Pitfield, D. Perrett, Comprehensive multi-dimensional liquid chromatographic  
561 separation in biomedical and pharmaceutical analysis: A review, *Biomed. Chromatogr.* 20 (2006)  
562 508–529. <https://doi.org/10.1002/bmc.672>.

563 [57] T. Murahashi, Comprehensive two-dimensional high-performance liquid chromatography for the  
564 separation of polycyclic aromatic hydrocarbons, *Analyst*. 128 (2003) 611–615.  
565 <https://doi.org/10.1039/b212643e>.

566 [58] N. Tanaka, H. Kimura, D. Tokuda, K. Hosoya, T. Ikegami, N. Ishizuka, H. Minakuchi, K.  
567 Nakanishi, Y. Shintani, M. Furuno, K. Cabrera, Simple and Comprehensive Two Dimensional  
568 Reversed-Phase HPLC Using Monolithic Silica Column, *Anal. Chem.* 76 (2004) 1273–1281.  
569 <https://doi.org/10.1021/ac034925j>.

570 [59] J.N. Fairchild, K. Horváth, G. Guiochon, Theoretical advantages and drawbacks of on-line,  
571 multidimensional liquid chromatography using multiple columns operated in parallel, *J.  
572 Chromatogr. A*. 1216 (2009) 6210–6217. <https://doi.org/10.1016/j.chroma.2009.06.085>.

573 [60] Y. Chen, L. Montero, O.J. Schmitz, Advance in on-line two-dimensional liquid chromatography  
574 modulation technology, *TrAC - Trends Anal. Chem.* 120 (2019) 115647.  
575 <https://doi.org/10.1016/j.trac.2019.115647>.

576 [61] S.R. Wilson, M. Jankowski, M. Pepaj, A. Mihailova, F. Boix, G. Vivo Truyols, E. Lundanes, T.  
577 Greibrokk, 2D LC separation and determination of bradykinin in rat muscle tissue dialysate with  
578 on-line SPE-HILIC-SPE-RP-MS, *Chromatographia*. 66 (2007) 469–474.  
579 <https://doi.org/10.1365/s10337-007-0341-4>.

580 [62] A. Mihailova, H. Malerød, S.R. Wilson, B. Karaszewski, R. Hauser, E. Lundanes, T. Greibrokk,  
581 Improving the resolution of neuropeptides in rat brain with on-line HILIC-RP compared to on-  
582 line SCX-RP, *J. Sep. Sci.* 31 (2008) 459–467. <https://doi.org/10.1002/jssc.200700257>.

583 [63] X. Gu, C. Deng, G. Yan, X. Zhang, Capillary array reversed-phase liquid chromatography-based  
584 multidimensional separation system coupled with MALDI-TOF-TOF-MS detection for high-  
585 throughput proteome analysis, *J. Proteome Res.* 5 (2006) 3186–3196.  
586 <https://doi.org/10.1021/pr0602592>.

587 [64] C. Liu, X. Zhang, Multidimensional capillary array liquid chromatography and matrix-assisted  
588 laser desorption/ionization tandem mass spectrometry for high-throughput proteomic analysis, *J.  
589 Chromatogr. A*. 1139 (2007) 191–198. <https://doi.org/10.1016/j.chroma.2006.11.019>.

590 [65] Z. Huang, G. Yan, M. Gao, X. Zhang, Array-Based Online Two Dimensional Liquid  
591 Chromatography System Applied to Effective Depletion of High-Abundance Proteins in Human  
592 Plasma, *Anal. Chem.* 88 (2016) 2440–2445. <https://doi.org/10.1021/acs.analchem.5b04553>.

593 [66] X. Wang, M. Gao, X. Zhang, Microliter-level multi-channel fraction collector for high-  
594 throughput separation system, *J. Chromatogr. A.* 1656 (2021) 462535.  
595 <https://doi.org/10.1016/j.chroma.2021.462535>.

596 [67] X. Wang, G. Yan, H. Zheng, M. Gao, X. Zhang, Strategy for high-throughput identification of  
597 protein complexes by array-based multi-dimensional liquid chromatography-mass spectrometry,  
598 *J. Chromatogr. A.* 1652 (2021) 462351. <https://doi.org/10.1016/j.chroma.2021.462351>.

599 [68] E. Davydova, P.J. Schoenmakers, G. Vivó-Truyols, Study on the performance of different types  
600 of three-dimensional chromatographic systems, *J. Chromatogr. A.* 1271 (2013) 137–143.  
601 <https://doi.org/10.1016/j.chroma.2012.11.043>.

602 [69] N. Abdulhussain, S. Nawada, P. Schoenmakers, Latest Trends on the Future of Three-  
603 Dimensional Separations in Chromatography, *Chem. Rev.* 121 (2021) 12016–12034.  
604 <https://doi.org/10.1021/acs.chemrev.0c01244>.

605 [70] T. Themelis, A. Amini, J. De Vos, S. Eeltink, Towards spatial comprehensive three-dimensional  
606 liquid chromatography: A tutorial review, *Anal. Chim. Acta.* 1148 (2021) 238157.  
607 <https://doi.org/10.1016/j.aca.2020.12.032>.

608 [71] B. Wouters, J. De Vos, G. Desmet, H. Terryn, P.J. Schoenmakers, S. Eeltink, Design of a  
609 microfluidic device for comprehensive spatial two-dimensional liquid chromatography, *J. Sep.  
610 Sci.* 38 (2015) 1123–1129. <https://doi.org/10.1002/jssc.201401192>.

611 [72] B. Wouters, E. Davydova, S. Wouters, G. Vivo-Truyols, P.J. Schoenmakers, S. Eeltink, Towards  
612 ultra-high peak capacities and peak-production rates using spatial three-dimensional liquid  
613 chromatography, *Lab Chip.* 15 (2015) 4415–4422. <https://doi.org/10.1039/c5lc01169h>.

614 [73] E. Davydova, S. Wouters, S. Deridder, G. Desmet, S. Eeltink, P.J. Schoenmakers, Design and  
615 evaluation of microfluidic devices for two-dimensional spatial separations, *J. Chromatogr. A.*  
616 1434 (2016) 127–135. <https://doi.org/10.1016/j.chroma.2016.01.003>.

617 [74] S. Jespers, S. Deridder, G. Desmet, A microfluidic distributor combining minimal volume,  
618 minimal dispersion and minimal sensitivity to clogging, *J. Chromatogr. A.* 1537 (2018) 75–82.  
619 <https://doi.org/10.1016/j.chroma.2018.01.029>.

620 [75] T. Adamopoulou, S. Nawada, S. Deridder, B. Wouters, G. Desmet, P.J. Schoenmakers,

621 Experimental and numerical study of band-broadening effects associated with analyte transfer in  
622 microfluidic devices for spatial two-dimensional liquid chromatography created by additive  
623 manufacturing, *J. Chromatogr. A.* 1598 (2019) 77–84.  
624 <https://doi.org/10.1016/j.chroma.2019.03.041>.

625 [76] T. Adamopoulou, S. Deridder, T.S. Bos, S. Nawada, G. Desmet, P.J. Schoenmakers, Optimizing  
626 design and employing permeability differences to achieve flow confinement in devices for spatial  
627 multidimensional liquid chromatography, *J. Chromatogr. A.* 1612 (2020) 460665.  
628 <https://doi.org/10.1016/j.chroma.2019.460665>.

629 [77] R. Ghosh, G. Chen, U. Umathewa, P. Gatt, A flow distribution and collection feature for ensuring  
630 scalable uniform flow in a chromatography device, *J. Chromatogr. A.* 1618 (2020) 460892.  
631 <https://doi.org/10.1016/j.chroma.2020.460892>.

632 [78] T. Adamopoulou, S. Deridder, G. Desmet, P.J. Schoenmakers, Two-dimensional insertable  
633 separation tool (TWIST) for flow confinement in spatial separations, *J. Chromatogr. A.* 1577  
634 (2018) 120–123. <https://doi.org/10.1016/j.chroma.2018.09.054>.

635 [79] T. Themelis, J. De Vos, J.L. Dores-Sousa, T. van Assche, S. Eeltink, Engineering solutions for  
636 flow control in microfluidic devices for spatial multi-dimensional liquid chromatography, *Sensors*  
637 *Actuators, B Chem.* 320 (2020) 128388. <https://doi.org/10.1016/j.snb.2020.128388>.

638 [80] S.H. Nawada, T. Aalbers, P.J. Schoenmakers, Freeze-thaw valves as a flow control mechanism in  
639 spatially complex 3D-printed fluidic devices, *Chem. Eng. Sci.* 207 (2019) 1040–1048.  
640 <https://doi.org/10.1016/j.ces.2019.07.036>.

641 [81] F. Erni, R.W. Frei, Two-dimensional column liquid chromatographic technique for resolution of  
642 complex mixtures, *J. Chromatogr. A.* 149 (1978) 561–569. [https://doi.org/10.1016/S0021-9673\(00\)81011-0](https://doi.org/10.1016/S0021-9673(00)81011-0).

644 [82] C.J. Venkatramani, Y. Zelechonok, An automated orthogonal two-dimensional liquid  
645 chromatograph, *Anal. Chem.* 75 (2003) 3484–3494. <https://doi.org/10.1021/ac030075w>.

646 [83] C.J. Venkatramani, A. Patel, Towards a comprehensive 2-D-LC-MS separation, *J. Sep. Sci.* 29  
647 (2006) 510–518. <https://doi.org/10.1002/jssc.200500341>.

648 [84] C.J. Venkatramani, Y. Zelechonok, Two-dimensional liquid chromatography with mixed mode  
649 stationary phases, *J. Chromatogr. A.* 1066 (2005) 47–53.  
650 <https://doi.org/10.1016/j.chroma.2004.11.103>.

651 [85] A.J. Alexander, L. Ma, Comprehensive two-dimensional liquid chromatography separations of

652 pharmaceutical samples using dual Fused-Core columns in the 2nd dimension, *J. Chromatogr. A.*  
653 1216 (2009) 1338–1345. <https://doi.org/10.1016/j.chroma.2008.12.063>.

654 [86] O.P. Haefliger, Universal two-dimensional HPLC technique for the chemical analysis of complex  
655 surfactant mixtures, *Anal. Chem.* 75 (2003) 371–378. <https://doi.org/10.1021/ac020534d>.

656 [87] Y. Fa, Y. Yu, F. Li, F. Du, X. Liang, H. Liu, Simultaneous detection of anions and cations in  
657 mineral water by two dimensional ion chromatography, *J. Chromatogr. A.* 1554 (2018) 123–127.  
658 <https://doi.org/10.1016/j.chroma.2018.04.017>.

659 [88] Q. Ren, C. Wu, J. Zhang, Use of on-line stop-flow heart-cutting two-dimensional high  
660 performance liquid chromatography for simultaneous determination of 12 major constituents in  
661 tartary buckwheat (*Fagopyrum tataricum* Gaertn), *J. Chromatogr. A.* 1304 (2013) 257–262.  
662 <https://doi.org/10.1016/j.chroma.2013.07.008>.

663 [89] S. Wang, L. Zhou, Z. Wang, X. Shi, G. Xu, Simultaneous metabolomics and lipidomics analysis  
664 based on novel heart-cutting two-dimensional liquid chromatography-mass spectrometry, *Anal.*  
665 *Chim. Acta.* 966 (2017) 34–40. <https://doi.org/10.1016/j.aca.2017.03.004>.

666 [90] S. Wang, Z. Wang, L. Zhou, X. Shi, G. Xu, Comprehensive Analysis of Short-, Medium-, and  
667 Long-Chain Acyl-Coenzyme A by Online Two-Dimensional Liquid Chromatography/Mass  
668 Spectrometry, *Anal. Chem.* 89 (2017) 12902–12908.  
669 <https://doi.org/10.1021/acs.analchem.7b03659>.

670 [91] W. Ma, S. Wang, T. Zhang, E.Y. Zhang, L. Zhou, C. Hu, J.J. Yu, G. Xu, Activation of choline  
671 kinase drives aberrant choline metabolism in esophageal squamous cell carcinomas, *J. Pharm.*  
672 *Biomed. Anal.* 155 (2018) 148–156. <https://doi.org/10.1016/j.jpba.2018.03.062>.

673 [92] W.C. Byrdwell, Breaking the rules: Two- and three-dimensional liquid chromatography with four  
674 dimensions of mass spectrometry, *Curr. Trends Mass Spectrom.* 19 (2021) 6–11.

675 [93] W.C. Byrdwell, H.K. Kotapati, R. Goldschmidt, P. Jakubec, L. Nováková, Three-dimensional  
676 liquid chromatography with parallel second dimensions and quadruple parallel mass spectrometry  
677 for adult/infant formula analysis, *J. Chromatogr. A.* 1661 (2022) 462682.  
678 <https://doi.org/10.1016/j.chroma.2021.462682>.

679 [94] C.J. Chen, F.A. Li, G.R. Her, Development of a low-flow multiplexed interface for capillary  
680 electrophoresis/electrospray ion trap mass spectrometry using sequential spray, *Electrophoresis.*  
681 29 (2008) 1997–2003. <https://doi.org/10.1002/elps.200700445>.

682 [95] E.A. Livesay, K. Tang, B.K. Taylor, M.A. Buschbach, D.F. Hopkins, B.L. LaMarche, R. Zhao, Y.

683 Shen, D.J. Orton, R.J. Moore, R.T. Kelly, H.R. Udseth, R.D. Smith, Fully automated four-column  
684 capillary LC-MS system for maximizing throughput in proteomic analyses, *Anal. Chem.* 80  
685 (2008) 294–302. <https://doi.org/10.1021/ac701727r>.

686 [96] K. Zhang, Y. Li, M. Tsang, N.P. Chetwyn, Analysis of pharmaceutical impurities using multi-  
687 heartcutting 2D LC coupled with UV-charged aerosol MS detection, *J. Sep. Sci.* 36 (2013) 2986–  
688 2992. <https://doi.org/10.1002/jssc.201300493>.

689 [97] J. Lin, C. Tsang, R. Lieu, K. Zhang, Fast chiral and achiral profiling of compounds with multiple  
690 chiral centers by a versatile two-dimensional multicolumn liquid chromatography (LC–mLC)  
691 approach, *J. Chromatogr. A.* 1620 (2020) 460897. <https://doi.org/10.1016/j.chroma.2020.460987>.

692 [98] H. Wang, H.R. Herderschee, R. Bennett, M. Potapenko, C.J. Pickens, B.F. Mann, I.A. Haidar  
693 Ahmad, E.L. Regalado, Introducing online multicolumn two-dimensional liquid chromatography  
694 screening for facile selection of stationary and mobile phase conditions in both dimensions, *J.*  
695 *Chromatogr. A.* 1622 (2020) 460895. <https://doi.org/10.1016/j.chroma.2020.460895>.

696 [99] C.J. Pickens, I.A. Haidar Ahmad, A.A. Makarov, R. Bennett, B.F. Mann, E.L. Regalado,  
697 Comprehensive online multicolumn two-dimensional liquid chromatography-diode array  
698 detection-mass spectrometry workflow as a framework for chromatographic screening and  
699 analysis of new drug substances, *Anal. Bioanal. Chem.* 412 (2020) 2655–2663.  
700 <https://doi.org/10.1007/s00216-020-02498-8>.

701 [100] L. Verscheure, G. Vanhoenacker, S. Schneider, T. Merchiers, J. Storms, P. Sandra, F. Lynen, K.  
702 Sandra, 3D-LC-MS with 2D Multimethod Option for Fully Automated Assessment of Multiple  
703 Attributes of Monoclonal Antibodies Directly from Cell Culture Supernatants, *Anal. Chem.* 94  
704 (2022) 6502–6511. <https://doi.org/10.1021/acs.analchem.1c05461>.

705

706 **Figure Captions**

707 **Figure 1.** Early demonstration of dual column array in the second dimension for the multiple heart-cut  
708 chiral-achiral 2D-LC analysis of stereoisomers of leucovorin (LV) and 5-methyltetrahydrofolate (5-  
709 METHF) in plasma. For the first 16.5 min after injection (panel A), eluent from the first dimension  
710 Resolvosil BSA-7 column was directed to waste (red trace) while <sup>2</sup>D column B is equilibrated (blue trace).  
711 Then, the *S* diastereomer of LV was loaded onto <sup>2</sup>D column A over the next six minutes (red trace in panel  
712 B). From 22.5 min to 46.5 min (panel C), an elution gradient was performed on <sup>2</sup>D column A (blue trace)  
713 while the *R* diastereomer of LV and both diastereomers of 5-METHF were loaded onto <sup>2</sup>D column B (red  
714 trace). In the final 24 min of the method, an elution gradient was performed on <sup>2</sup>D column B (same position  
715 as panel A). Adapted from reference [37] with permission from Elsevier (Copyright 1990).

716

717 **Figure 2.** Schematic of a SEC-RPLC-UV-MS technique using a dual <sup>2</sup>D column array with two switching  
718 valves. Reproduced from reference [39] with permission from the American Chemical Society (Copyright  
719 1997).

720

721 **Figure 3.** Instrument diagram for the IEX-RPLC-UV separation of peptides and small proteins with  
722 fraction collection for offline MALDI-MS analysis. This system included four identical RP columns in  
723 the <sup>2</sup>D array. Reproduced from reference [44] with permission from the American Chemical Society  
724 (Copyright 2002).

725

726 **Figure 4.** Schematic of a 2D IEX-RPLC separation for the analysis of intact proteins using a <sup>2</sup>D array of  
727 twelve columns connected to two selector valves. Reproduced from reference [47] with permission from  
728 Elsevier (Copyright 2018).

729

730 **Figure 5.** 2D contour plot for NPLC x RPLC separation using dual <sup>2</sup>D column. Peak capacity of 487 was  
731 obtained in this mixture of 28 standard compounds. Reproduced from reference [50] with permission from  
732 Elsevier (Copyright 2008).

733

734 **Figure 6.** Schematic of a 2D SCX-RPLC system with a <sup>2</sup>D array of 18 capillary. These columns elute  
735 onto a MALDI plate for offline MALDI-TOF-TOF-MS detection. Adapted from reference [63] with  
736 permission from the American Chemical Society (Copyright 2006).

737

738 **Figure 7.** Microfluidic device with a single  $^1\text{D}$  column channel, a  $^2\text{D}$  flow distributor, 21 parallel  $^2\text{D}$   
739 column channels, and an outlet flow collector. Reproduced from reference [71] with permission from John  
740 Wiley and Sons (Copyright 2015).

741

742 **Figure 8.** 2D contour plots for the 2D-LC separation of a test mixture of aromatic compounds. The  $^1\text{D}$   
743 ODS-AQ column eluent was sampled onto cyano and amino  $^2\text{D}$  columns in an alternating sequence.  
744 Reproduced from reference [82] with permission from the American Chemical Society (Copyright 2003).

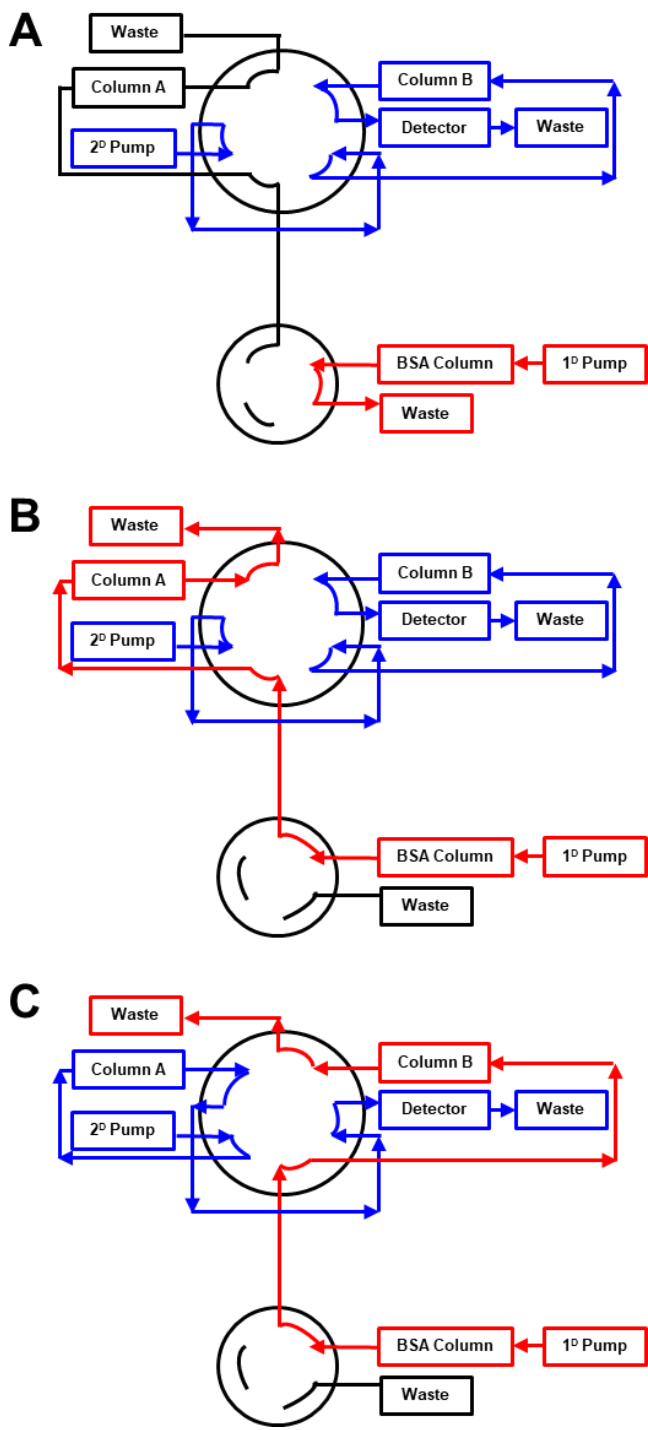
745

746 **Figure 9.** Schematic of an achiral-chiral 2D-LC separation with six  $^2\text{D}$  chiral columns for automated  
747 column screening during method development. Reproduced from reference [97] with permission from  
748 Elsevier (Copyright 2020).

749

750 **Figures**

751 **Figure 1.**



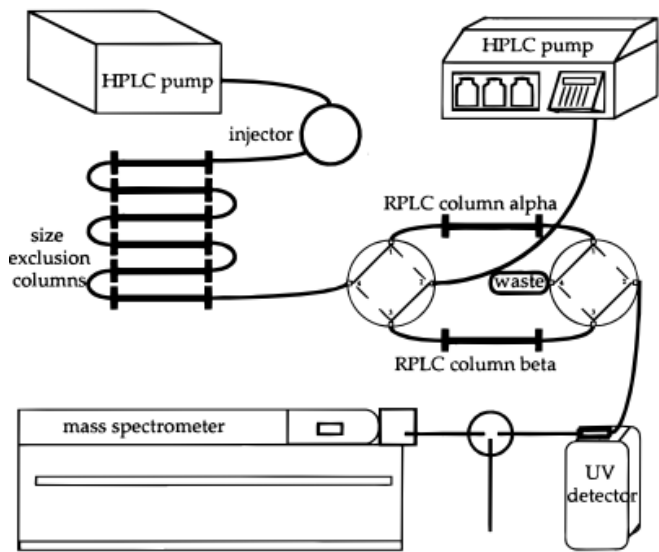
752

753

754

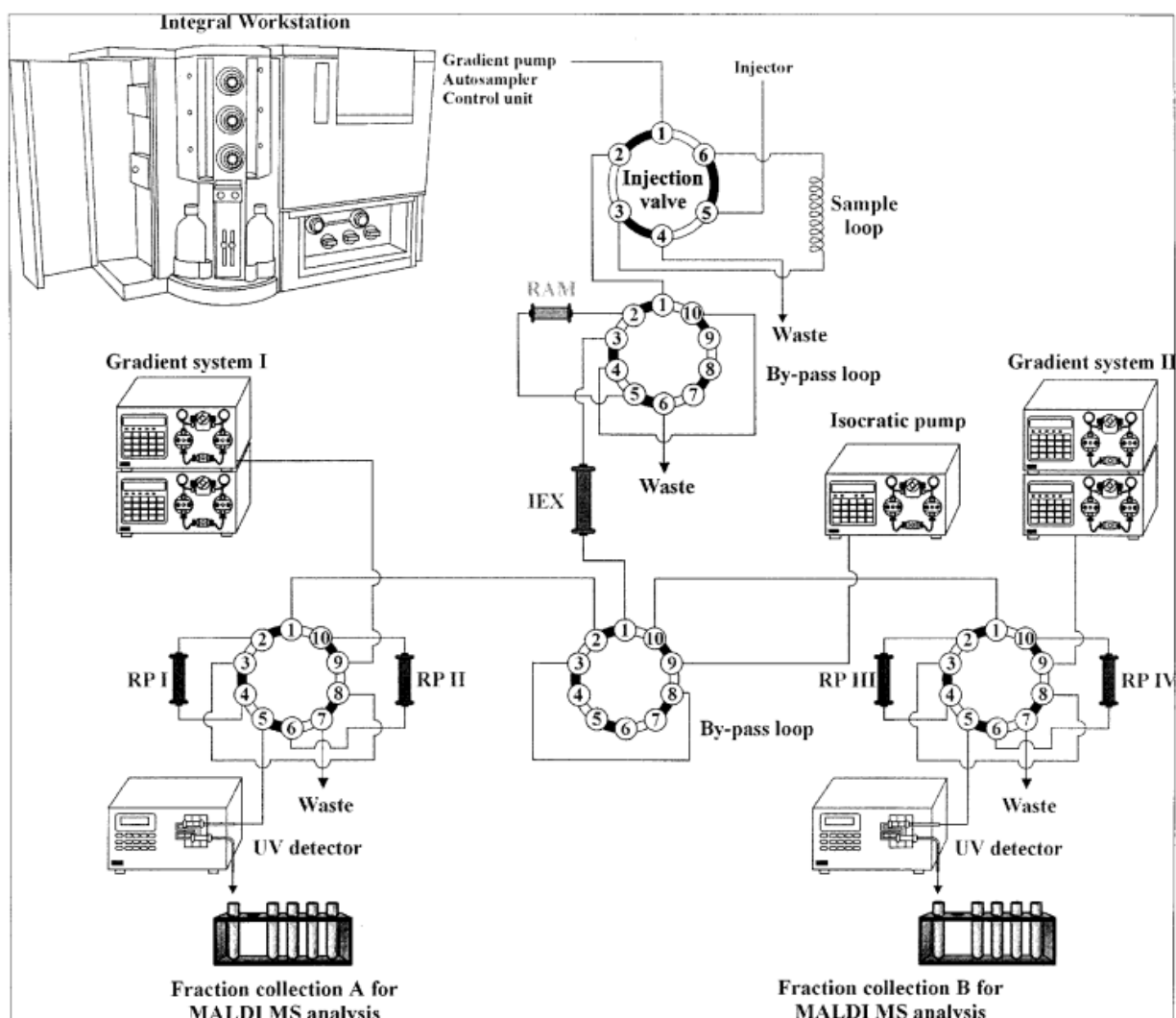
755

**Figure 2.**

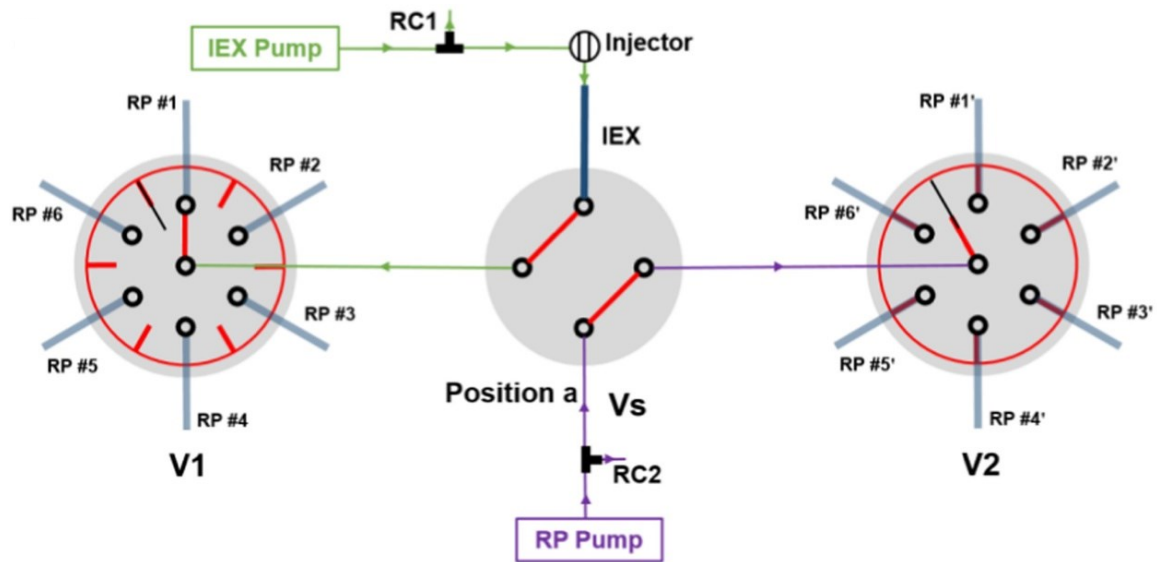


756

757

**Figure 3.**

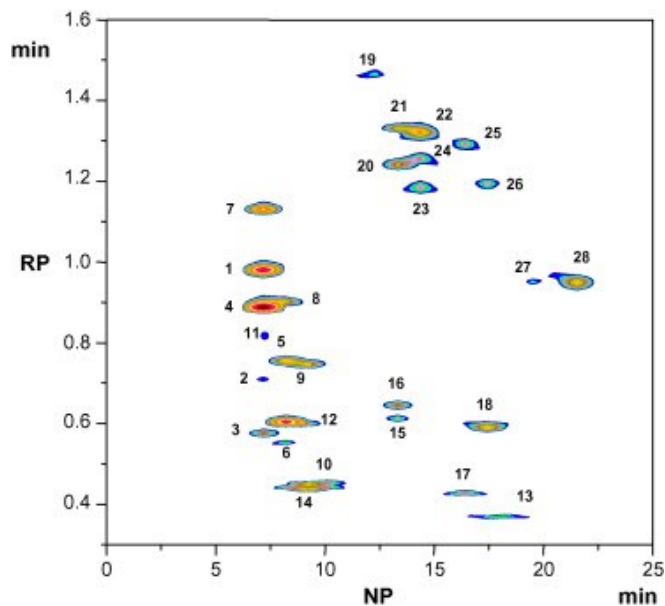
761 **Figure 4.**



762

763

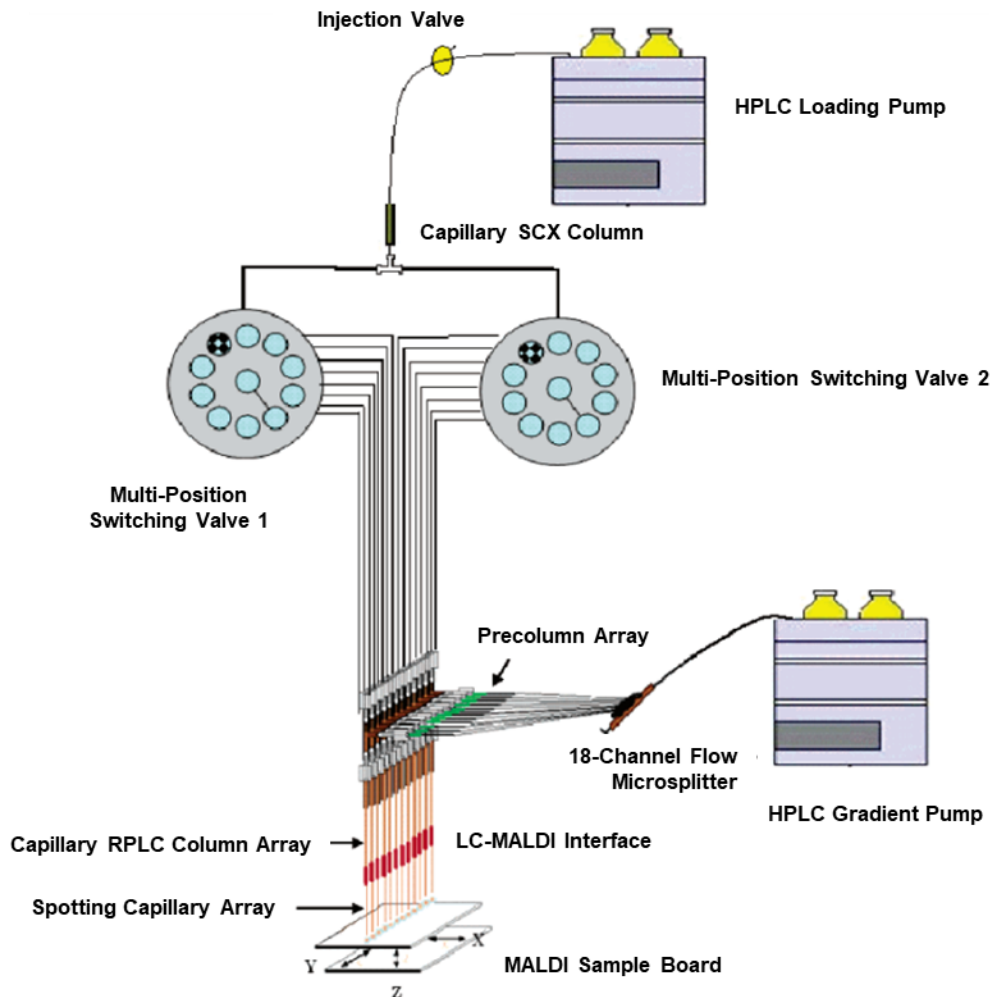
764

**Figure 5.**

765

766

767 **Figure 6.**



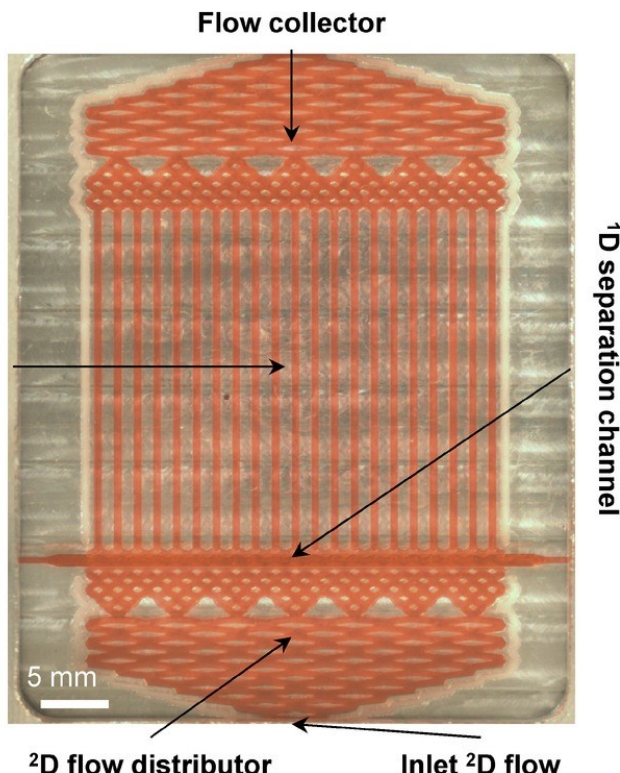
768

769

770

Figure 7.

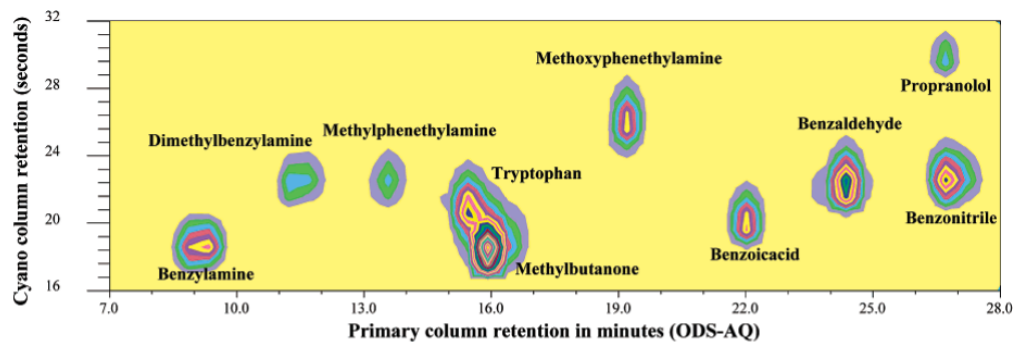
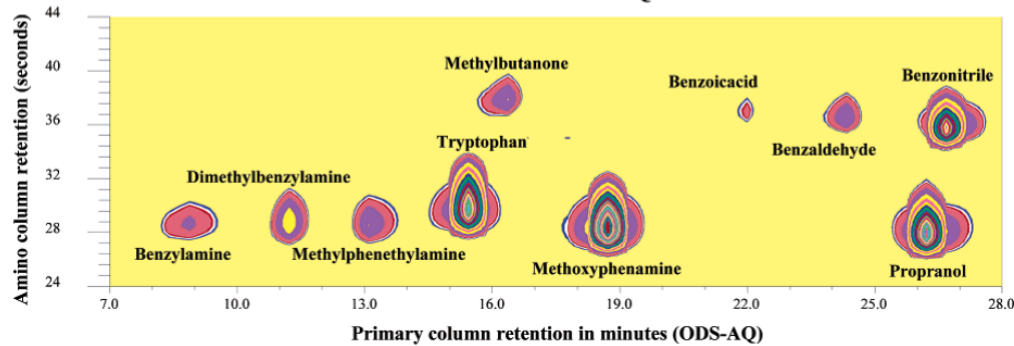
21<sup>2D</sup> separation channels



771

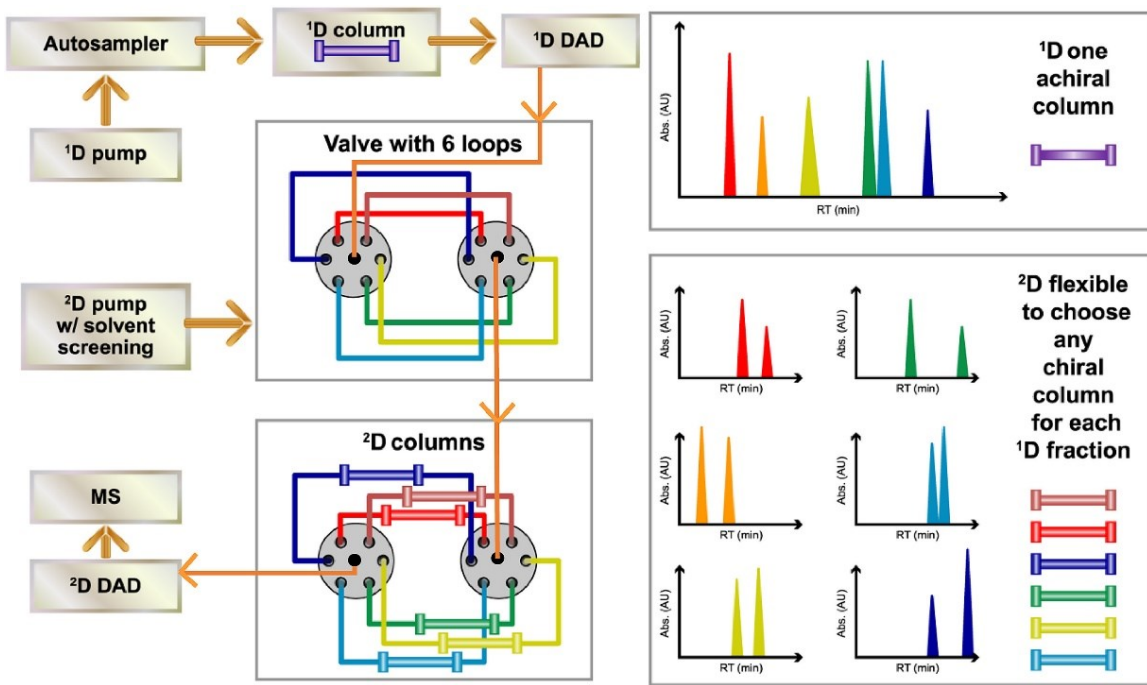
772

773

**Figure 8.****2D-LC of test mixture on ODS-AQ/Cyano column****2D-LC of test mixture on ODS-AQ/Amino column**

777

Figure 9.



778

779

780

781 **Table 1.** Summary of Parallel Column Arrays Operated in an Alternating or Sequential Order

<u>Method Designation</u>	<u>1D Column(s)</u>	<u>2D Columns</u>	<u>Modulation Scheme</u>	<u>Sample Description</u>	<u>Total Separation Time</u>	<u>Peak Capacity</u>	<u>Reference</u>
Multiple heart-cut	Resolvosil BSA-7 (4 mm x 150 mm)	Two LiChrocart RP-18 (4 mm x 125 mm)	10-port valve	Pharmaceutical drugs in extracted plasma	71.5 min	N.R.	[37]
Comprehensive	G2000SW <sub>XL</sub> (7.8 mm x 300 mm, six coupled serially)	Two Micra RP-18 (4.6 mm x 33 mm)	Two 4-port valves	Tryptic digest of ovalbumin	180 min	495	[39]
Comprehensive	G2000SW <sub>XL</sub> (7.8 mm x 300 mm, six coupled serially)	Two Hypersil BDS C-18 (1.0 mm x 20 mm)	Two 4-port valves	Tryptic digest of bovine serum albumin	320 min	520	[40]
Comprehensive	G3000SW <sub>XL</sub> (7.8 mm x 300 mm, eight coupled serially)	Two PerSeptive R2/H (2.1 mm x 33 mm)	Two 4-port valves	Protein mixture ( <i>E. coli</i> lysate)	390 min	N.R.	[41]
Comprehensive	G3000SW <sub>XL</sub> & G4000SW <sub>XL</sub> (7.8 mm x 300 mm, six of each coupled serially)	Two PerSeptive R2/H (2.1 mm x 100 mm)	Two 4-port valves	Protein mixture ( <i>E. coli</i> lysate)	1050 min	1500	[41]
Comprehensive	TSK-gel DEAE-NPR or TSK-gel SP-NPR (4.6 mm x 35 mm)	Two Micra NPS ODS I (4.6 mm x 14 mm)	10-port valve	Standard protein mixture and human fibroblast cell extract	20 min	600	[42],[43]

Comprehensive	TSK-gel DEAE-NPR or TSK-gel SP-NPR (4.6 mm x 35 mm)	Four Micra NPS ODS I (4.6 mm x 14 mm)	Three 10-port valves	Human hemofiltrate (including from chronic renal patients) and human fibroblast cell lysate (20 kDa cutoff)	96 min	3000	[44],[45]
Comprehensive	Co-polymer monolith functionalized with tertiary amine groups (0.250 mm x 260 mm)	Three PS-DVB monolith (0.250 mm x 260 mm)	Two 7-port selector valves	Protein mixtures (Standards & <i>E. coli</i> lysate)	630 min	N.R.	[46]
Comprehensive	Co-polymer monolith functionalized with tertiary amine groups (0.250 mm x 300 mm)	Twelve PS-DVB monolith (0.250 mm x 300 mm)	Two 7-port selector valves & one 4-port valve	Protein mixtures (Standards & <i>E. coli</i> lysate)	252 min	N.R.	[47]
Comprehensive	BioBasic AX (4.6 mm x 250 mm)	Two (plus one additional in series) SinoChrom ODS-BP (4.6 mm x 50 mm)	10-port valve	Tryptic digest of standard protein mixture	100 min	650 (890 at high temp. conditions)	[49]
Comprehensive	Betasil Diol (1.0 mm x 250 mm)	Two Zorbax SB C18 (4.6 mm x 50 mm)	Two 10-port valves	Small molecule test mixture	25 min	516 (487 corrected for complementarity)	[50]
Comprehensive	Betasil Diol	Two	Two	Lemon oil extract	90 min	1840	[50]

	(1.0 mm x 250 mm)	Zorbax SB C18 (4.6 mm x 50 mm)	10-port valves			(1095 corrected for complementarity)	
Comprehensive	Zorbax SB CN (2.1 mm x 150 mm)	Two Zorbax SB C18 (4.6 mm x 50 mm)	Two 10-port valves	Steroid mixture	25 min	400 (82 corrected for complementarity)	[50]
Comprehensive	Zorbax SB CN (2.1 mm x 150 mm)	Two Zorbax SB C18 (4.6 mm x 50 mm)	Two 10-port valves	Sulfonamide mixture	75 min	N.R.	[50]
Comprehensive	Zorbax SB CN (2.1 mm x 150 mm)	Two Zorbax SB C18 (4.6 mm x 50 mm)	Two 10-port valves	Phenacyl esters of triglycerides in fish oil	60 min	290 (159 corrected for complementarity and 90 corrected for complementarity and undersampling)	[51]
Comprehensive	Halo C18 (2.1 mm x 150 mm, four coupled serially, low pH)	Two Zorbax 300 Extend ODS (4.6 mm x 50 mm, high pH)	Two 10-port valves	Tryptic digests of bovine serum albumin and human serum	360 min	4677 (corrected for complementarity and undersampling)	[52]
Comprehensive	Discovery HS PEG (4.6 mm x 150 mm)	Two Discovery ZR-CARBON (2.1 mm x 50 mm)	10-port valve	Standard mixture of phenolic compounds and flavonoids, beer	135 min	N.R.	[53]

Comprehensive	Discovery HS PEG (2.1 mm x 50 mm) & Purospher Star RP-18e (4.6 mm x 150 mm) connected in series	Two Discovery ZR-CARBON (2.1 mm x 50 mm)	10-port valve	Standard mixture of phenolic compounds and flavonoids, beer	160 min	N.R.	[53]
Comprehensive	Zorbax SB C18 (0.5 mm x 150 mm)	Two Discovery ZR-CARBON (2.1 mm x 50 mm)	10-port valve	Standard mixture of phenolic compounds and alkylbenzenes, beer, wine	130 min	N.R.	[54]
Comprehensive	Shodex SP-420N (4.6 mm x 35 mm)	Two Eichrom NPS C18 (4.6 mm x 33 mm)	10-port valve	Standard protein mixture	84 min	N.R.	[55]
Comprehensive	Shodex SP-420N (4.6 mm x 35 mm)	Two Symmetry300 C4 (2.1 mm x 50 mm)	10-port valve	Ribosomal proteins (yeast cell lysate)	200 min	~700	[55]
Comprehensive	SCX-SAX columns coupled in series	Two ODS monolith	6-port valve	Human urinary metabolites	160 min	N.R.	[56]
Comprehensive	Cosmosil 5PBB (4.6 mm x 150 mm)	Two Chromolith SpeedROD (4.6 mm x 50 mm)	10-port valve	Polycyclic aromatic hydrocarbons (standards and from gasoline extract)	30 min	N.R.	[57]
Comprehensive	Fluofix (4.6 mm x 150 mm)	Two ODS monolith	Flow switch and two	Standard mixture of hydrocarbons	65 min	1190	[58]

		(4.6 mm x 30 mm)	6-port valves	and benzene derivatives			
Comprehensive	Waters ODS-AQ (4.6 mm x 150 mm)	Two Exsil Amino (4.6 mm x 50 mm)	12-port valve	Small molecule standard test mixture	30 min	450	[82]
Comprehensive	X-Terra C18 (4.6 mm x 150 mm)	Two Zorbax SB-Phenyl (4.6 mm x 50 mm)	12-port valve	Small molecule drug mixture	35 min	N.R.	[83]
Comprehensive	Zorbax Extended C18 (2.1 mm x 150 mm)	Ascentis Express C18 (3.0 mm x 50 mm)	12-port valve	Mixture of drug degradants	17 min	N.R.	[85]

782

783

**Table 2.** Summary of Parallel Column Arrays Operated Simultaneously

<u>Method Designation</u>	<u>1D Column</u>	<u>2D Columns</u>	<u>Modulation Scheme</u>	<u>Sample Description</u>	<u>Total Separation Time<sup>a</sup></u>	<u>Number of Protein Identifications</u>	<u>Reference</u>
Comprehensive	POROS SCX (0.53 mm x 150 mm)	18 Hypersil C18 (0.25 mm x 250 mm)	Two 11-port selector valves	Tryptic digest of proteins from human liver tissue	180 min	462	[63]
Comprehensive	POROS SCX (0.32 mm x 70 mm)	10 Zorbax 300 SB C8 (0.25 mm x 250 mm)	In-house fabricated multiple-channel interface	Tryptic digest of proteins from liver cancer tissue (from mouse model)	150 min	1202	[64]
Multiple heart-cut	ProPac SAX-10 (4.0 mm x 250 mm)	Eight Xtimate C8 (2.1 mm x 250 mm)	11-port selector valve	Proteins in human plasma	240 min	1332	[65]
Multiple heart-cut	PolyCATWAX50/50 (4.6 mm x 200 mm)	Eight UniPS 5-1000 SS (2.1 mm x 150 mm)	11-port selector valve	HeLa cell lysate	300 min	4436	[67]

<sup>a</sup> Times listed for primary 2D-LC separation and do not include additional off-line detection time by MS or LC-MS.

**Table 3.** Summary of Parallel Column Arrays with Different <sup>2</sup>D Stationary Phases

<u>Method Designation</u>	<u>1D Column(s)</u>	<u>2D Columns</u>	<u>Modulation Scheme</u>	<u>Sample Description</u>	<u>Total Separation Time</u>	<u>Reference</u>
Comprehensive	Waters ODS-AQ (4.6 mm x 150 mm)	Exsil Amino (4.6 mm x 50 mm) & Platinum Cyano (7.0 mm x 33 mm)	12-port valve	Standard mixture of small molecule aromatic compounds	30 min	[82]
Comprehensive	Primesep-100 (4.6 mm x 150 mm)	Primesep-100 (4.6 mm x 20 mm) & Primesep-B (4.6 mm x 20 mm)	12-port valve	Small molecule standard test mixture	30 min	[84]
Comprehensive	Primesep-B (4.6 mm x 150 mm)	Primesep-100 (4.6 mm x 20 mm) & Primesep-B (4.6 mm x 20 mm)	12-port valve	Small molecule standard test mixture	30 min	[84]
Multiple heart-cut	Nucleosil 100-5 OH (1.0 mm x 250 mm)	Nucleosil 120-5 C4 (4.0 mm x 125 mm) & Nucleosil 100-7 C2 (4.0 mm x 250 mm)	10-port valve	Complex surfactant mixture	54 min	[86]
Multiple heart-cut	Thermo Carbohydrate Removal Cartridge (2.0 mm x 150 mm) or IonPac CG12A (2.0 mm x 50 mm)	IonPac CS12A (2.0 mm x 250 mm) & IonPac AS11-HC (2.0 mm x 250 mm)	10-port valve	Standard mixture of inorganic ions and mineral water samples	25 min	[87]

Comprehensive	Fluofix (4.6 mm x 150 mm)	One ODS monolith and one PBB monolith (both 4.6 mm x 30 mm)	Flow switch and two 6-port valves	Standard mixture of hydrocarbons and benzene derivatives	65 min (130 min if run twice for full coverage)	[58]
Multiple heart-cut (with stop flow)	Acclaim Mixed- Mode HILIC-10 (2.1 mm x 10 mm)	Acclaim RSLC Polar Advantage II (2.1 mm x 150 mm) & Acclaim RSLC Phenyl-1 (2.1 mm x 150 mm)	10-port valve & 6-port valve	Small molecules from tartary buckwheat plants	75 min	[88]
Multiple heart-cut	Acquity BEH C8 (2.1 mm x 5 mm)	Acquity BEH C18 (2.1 mm x 50 mm or 2.1 mm x 100 mm) & Acquity HSS T3 (2.1 mm x 50 mm)	6-port valve, 8-port valve, & 10-port valve	Pooled plasma, mouse tissue liver extract, prostate cancer cells, serum from esophageal squamous cell carcinoma patients	30 min	[89], [90], [91]
Comprehensive (split-flow, multicycle)	Two Inertsil ODS-2 (4.6 mm x 250 mm) connected in series	Two Accucore C30 (2.1 mm x 50 mm & 3.0 mm x 100 mm)	Prototype valve switching system	Infant/adult nutritional formula	75 min	[92], [93]
Multiple heart-cut	XTerra RP18 (4.6 mm x 150 mm) or	Six assorted RP and HILIC columns (varying dimensions)	Two 6-port valves &	Pharmaceutical compound (peak purity profiling)	10 – 25 min	[96]

(with peak parking)	Zorbax Eclipse XDB C18 (4.6 mm x 150 mm)		four 7-port selector valves			
Multiple heart-cut	Ascentis Express C18 (4.6 mm x 150 mm) Or Poroshell EC-C18 (3.0 mm x 150 mm)	Six polysaccharide chiral phases (all 3.0 mm x 50 mm)	Four 7-port selector valves	Pharmaceutical compound (chiral purity profiling)	24 min	[97]
Multiple heart-cut	Six RP columns (all 2.1 mm x 50 mm)	Four chiral phase columns (all 4.6 mm x 50 mm)	Two 14-port, 6-position column selection valves & 8-port duo head valve	Pharmaceutical compound (chiral purity profiling)	<20 min	[98]
Comprehensive	C4, SEC, SAX, and SCX columns (various dimensions)	Three RP columns (all 3.0 mm x 50 mm)	Two 14-port, 6-position column selection valves & 8-port duo head valve	Standard protein mixture (both intact and chymotryptic digest)	<35 min	[99]
Multiple heart-cut	Bio-Monolith Protein A column (5.2 mm x 5 mm)	AdvanceBio SEC 300A (7.8 mm x 300 mm), Bio Mab NP5 PK	10-port active solvent modulation valve & two 8-port duo head valves	Monoclonal antibodies	<70 min (includes <sup>3</sup> D desalting SEC column)	[100]

		(2.1 mm x 250 mm, or alternate MabPac SCX-10), AdvanceBio HIC (4.6 mm x 100 mm)				
--	--	---	--	--	--	--